TALLINN UNIVERSITY OF TECHNOLOGY
TARTU COLLEGE

Department of sustainable technology

HYBRID NANOMATERIALS BASED ON CARBON NANOTUBES AND METAL OXIDE NANOPARTICLES FOR PHOTOVOLTAIC APPLICATIONS

SÜSINIKNANOTORUDEL JA METALLOKSIID NANOOSAKESTEL PÕHINEVAD NANOHÜBRIIDMATERJALID FOTOELETRILISTEKS RAKENDUSTEKS

Master thesis

Environmental engineering

Undergraduate: Martin Salumaa

Supervisor: Prof. Erwan Rauwel

Co-supervisor: Dr. Protima Rauwel

Tartu 2015

Hereby I declare that this master thesis is my original investigation and achievement. All used materials of other authors, important statements from literature or somewhere else originated data in this thesis are referred.

……...…….. (signature of the author, date)
Code: 092640EAKI

Master thesis corresponds to the requirements

…… (signature of the supervisors, date)

Allowed to the defence: ……..……..…… (date)

Chairperson of the defence committee: ……..……..... (date)

ABSTRAKT

Käesoleva uurimusliku teadustöö, mille pealkiri on „Süsiniknanomaterjalidel ja metalloksiidide nanoosakestel põhinevad nanohübriid materjalid fotoelektrilisteks rakendusteks“, autor on Martin Salumaa ning selle alusel taotletakse tehnikateaduste magistrikraadi. Uurimustöö on kirjutatud aastal 2015 Tallinna Tehnikaülikooli Tartu Kolledžis. Töö koosneb kahest köitest, 65 leheküljest, 3 tabelist, 27 joonisest/pildist ja 75 viitest. Töö on kirjutatud inglise keeles.

Töö eesmärkideks oli uurida süsiniknanotorude (CNT) ja hafniumdioksiidi nanohübriidmaterjali sünteesimise protessi ja eelnimetatud hübriidmaterjali fotoelektrilisi omadusi. Püstitatud eesmärkide täitmiseks viidi läbi järgmised toimingud:

1. Viidi läbi ulatuslik kirjanduse uurimine süsiniknanotorudest, metalloksiid nanoosakestest ja hübriidmaterjalidest, mis koosnevad süsiniknanotorudest ja metalloksiid nanoosakestest.
2. Koostati kirjanduse ülevaade punktis 1 nimetatud materjalide kohta.
3. Valmistati süsiniknanotoru – hafniumdioksiid nanohübriid ultrahelitöötluse teel.
4. Valmistatud nanohübriidmaterjali uuriti transmissioon-elektronmikroskoobiga.
5. Uuriti ja iseloomustati ultraheli mõju süsiniknanotorude hajususele etanoolis.
6. Uuriti ja iseloomustati ultraheli mõju hafniumdioksiidi nanoosakeste hajususele ja aglomeratsioonile etanoolis.
7. Uuriti ja iseloomustati ultraheli tekitatud kahjustusi süsiniknanotorudele.
8. Viidi läbi elektrilised mõõtmised iseloomustamaks valmistatud materjali elektrilisi ja fotoelektrilisi omadusi.

Käesoleva töö esimene pool sisaldab kirjanduse ülevaadet süsininanotorude füüsikalistest, keemilistest, optilistest ja elektrilistest omadustest; ja metalloksiid nanoosakestest ja nanohübriidmaterjalidest. Puudutatud on ka nanotorude ja nanoosakeste toksilisust ja ohtu tervisele.

Töö teine pool koosneb metoodika kirjeldusest, kasutatud materjalide ja uurimismeetodite kirjeldusest. Sellele järgneb ekperimentide kirjeldus, läbiviimise kord, tulemused ja arutelu.

Töö algusfaasis valmistati süsiniknanotoru – hafniumdioksiid nanohübriid kasutades lihtsat ultraheli töötluse meetodit. Kasutati 10.8 mg mitmeseinalisi süsiniknanotorusid ja 10.32 mg kuubikvõrega hafniumdioksiidi nanoosakesi, mille valmistas töö juhendaja prof. E.Rauwel. Hübriidmaterjali uurimisel kõrge resolutsiooniga transmissioon elektronmikroskoobis järeldati, et ultraheli on tõhus vahend osakeste hea hajususe saavutamiseks lahuses ja süsniknanotorude funktsionaliseerimiseks, millega tagati ka osakeste kinnitumine nanotorudele. Lisaks leiti, et ultraheli kestvusel on otsene mõju materjalide hajususele ja osakeste kinnitumisele – pikemat aega tööteldud materjali proovid näitasid ühtlasemat hajusust ja rohkem kinnitunud osakesi.

Sünteesiprotessis kasutatud materjalide kontsentratsiooni leidmiseks teostati arvutused. Selgus, et kasutatud materjalikogustega on teoreetiliselt võimalik saavutada nanotorude katmine nanoosakestega 19.1% ulatuses. Arvutusi saab edasises uurimustöös kasutada sünteesiprotsessi parameetrite optimeerimise eesmärgil.

Töö autor osales Eesti ja Prantsusmaa vahelises koostööprogrammis „G. – F. Parrot“, mille eesmärk on noorteadlaste kaasamine materjaliteaduse, nanotehnoloogia, robootika, IT ja keskonnateaduse teadusuuringutes. Sellest tulenevalt toimus nanohübriidi elektriliste omaduste selgitamise katsed Prantsusmaal, Grenobles, Minatec LAHC laboris. Kohapealne juhendaja oli dr. Frederique Ducroquet. Tulemused näitasid, et valmistatud materjal on väga tõhus elektrijuht isegi pärast intensiivet ultahelitöötlust. Lisaks tõendati, et materjalil on fotoelektrilised omadused, mis väljenduvad UV kiirguse mõjus elektrijuhtivusele, Materjal näitas ka elektrimahutuvust, mis kutsuti esile samuti UV kiirgusega.

Läbiviidud katsete tulemustest saab järeldada, et ultraheli on tõhus ja lihtne viis kõnealuse hübriidmaterjali valmistamiseks. Samuti seda, et süsiniknanotoru – hafniumdioksiid nanohübriid kätkeb endas fotoelektrilis omadusi. Siiski on vajalik edasine teadustöö, et materjali valmistamise protsessi täiustada ja saavutada paremad elektrilised omadused.

Märksõnad: metalloksiidnanoosakesed, süsiniknanotorud, nanohübriid, ultraheli, TEM

TABLE OF CONTENTS

ACRONYMS AND ABBREVIATIONS

1.	Å	Angstrom
2.	AFM	Atomic force microscopy
3.	Atm	Atmosphere
4.	CCVD	Catalytic carbon vapor deposition
5.	CNT	Carbon nanotube
6.	dV	Difference of voltage
7.	FCC	Face centered cubic
8.	GPa	Gigapascal
9.	HfO_2	Hafnium dioxide
10.	HRTEM	High resolution transmission electron microscope
11.	K	Kelvin
12.	kV	Kilovolt
13.	MPa	Megapascal
14.	MWCNT	Multi-walled carbon nanotube
15.	NP	Nanoparticle
16.	SSA	Specific surface area
17.	SWCNT	Single-walled carbon nanotube
18.	TEM	Transmission electron microscope
19.	TGA	Thermogravimetric
20.	TPa	Terapascal
21.	UV	Ultra violet
22.	XRD	X-ray diffraction

1. INTRODUCTION

1.1. Nanotechnology

The word ”nano” is derived from Greek *νᾶνος* (*nanos*) which means ”dwarf”. Nano is an official SI unit prefix and corresponds to one billionth (10^{-9}) of a meter. The word technology is derived from the Greek word *τέχνη* (*techne*), meaning art or skill, and *λογία (logia)* meaning science. Nanotechnology can then be described as the science of very small objects. However today, such a simple definition is not enough as the field of nanotechnology is growing rapidly and further restricting the meaning of ”nano”. It was not until the talk of American physicist Richard Feynman entitled ‘There’s plenty of room at the bottom’ [1] that the concept of nanotechnology took a leap. Feynman spoke about manipulating materials at the molecular level, even at an atomic scale and about the advantages of going small. At that time (1959) it was not yet possible to see individual atoms because the transmission electron microscopes were not powerful enough. Nevertheless, Feynman’s talk was one of the motivations for developing advanced scientific devices for the characterization of the materials at the nanoscale.

Nowadays, the most commonly agreed definition is the following: Nanotechnology is the understanding and control of matter at dimensions between approximately 1 and 100 nanometers, where unique phenomena enable novel applications. Encompassing nanoscale science, engineering, and technology, nanotechnology involves imaging, measuring, modeling, and manipulating matter at this length scale. ‘‘The most important requirement is that the nanomaterials have different properties than their bulk counterparts [2].

Nanotechnology is still not yet completely understood by the wider public and thus people have misinterpreted it. The main purpose of nanotechnology is to make more effective use of materials, to cure mortal diseases, to find alternative energy sources in order to satisfy ever-growing energy demands and subsequently cut down on fossil fuel consumption, which will effectively reduce the pollution.

The growth of nano-industry is reflected by the exponential rise of research funding. Nanotechnology research funds in the US have risen from 225 million USD in 2001 [3] to 1.5 billion USD in 2014 [4]. European 7^{th} framework program (2007 – 2013) provides funds of 3.5 billion € [5]. According to the latest NNI report, most of the funds are taken by fundamental research (34%), followed by applications (26%), infrastructure (16%) and

environment (7%) [4], an estimated total of 250 billion USD will have been invested in nanotechnology by the year 2015 [6].

Solutions based on Nanotechnology are promising to solve many economic, social and ecological problems of the modern society. These new solutions will also enhance the performances of existing technologies and improve other areas of science and research. The main challenges in the field of nanotechnology are to make it suitable for the health industry and overcome the cost barriers to make medical treatment available to everyone in need. Another priority is to relieve the pressure on environment due to growing population. In the field of water cleaning, nanotechnology offers new efficient methods for water purification and making clean water available to everyone. Nanotechnology also offers some solutions for the problem of energy demand with the development of green solutions. Nanotechnology solutions are also expected to improve information technology by further miniaturization and by finding more effective materials for existing transistors and computer chips. NASA is currently looking for new solutions based on nanotechnology for making the space exploration more feasible [7,8].

1.2. Carbon nanotubes and nanoparticles in nanotechnology

The progress made so far has been possible by the development of new nano-objects and carbon nanotubes (CNTs). A carbon nanotube is form of carbon stronger than steel and with excellent electrical and thermal conductivity. CNTs are of fundamental importance in the field of nanotechnology and are employed in many applications [9]. Another important family of nanomaterials is the metal oxide nanoparticles that are used for example in energy storage (RuO_2 for super capacitors) [10] or water purification (TiO_2 photo catalysts for degrading pollutants) [11]. The combination of CNTs with metal oxide nanoparticles and making them work together should enable to develop a new family of nanohybrid materials that may present new properties. CNTs and metal oxide nanoparticles and their field of applications will be further discussed in this manuscript.

1.3. CNT/HfO_2 nanoparticles based hybrid materials

The focus of this Masters' thesis is to study a new nanohybrid composite of CNTs mixed with HfO_2 nanoparticles for possible applications in photovoltaics and energy production. The growing demand for energy along with an exponential increase of the human population are draining fossil fuel resources that will soon not be sufficient for sustaining mankind's' needs. Alternative energy production is then necessary, but is still in its infancy with low efficiency factors.

The structure of this thesis consists firstly of a literature overview of CNTs and more particularly multi-walled carbon nanotubes (MWCNTs) and metal oxide nanoparticles. The present development of nanohybrids based on the combination of CNTs with metal oxide nanoparticles will also be discussed. The second part will describe the experiments and methodology that were used in this research project. The last part of the manuscript will describe the results and discuss the properties of these materials for photovoltaic applications.

2. State of the Art

2.1. Carbon nanotubes – CNTs and Graphene

Carbon nanotubes have been one of the most intensively investigated material during the last two decades [12]. To understand the structure of CNTs, it is necessary to understand graphene. Graphene is a single atom thick sheet of graphite, which is a crystalline form of carbon, with outstanding mechanical and electrical properties. The CNTs are sheets of graphene rolled up into tubes and CNTs can, according to the number of graphene sheets, be single-walled (SWCNTs) or multi-walled (MWCNTs). CNTs have highlighted the field of nanotechnology like no other materials previously. Their unique properties offer the possibility of developing applications that were not possible to develop before their discovery. The development of integrated circuits, memory devices, gas sensors, solar cells and even space elevators are good examples of what was developed and will be developed in the future [13].

2.2. Discovery of CNTs

The discovery of CNTs has been attributed to Sumio Iijima who described them first in 1991. CNTs had actually been somewhat observed earlier by many scientists who were trying to understand their formation mechanism to prevent them from forming in steel processing and in coolant tubes of nuclear reactors, however, earlier papers were lacking scientific credibility due to low magnification images and conclusions drawn from diffraction patterns. For example, first report of tubular carbon filaments in the Journal of Physical Chemistry of Russia appeared in 1952. In 1958 carbon filaments were reported to exhibit the concentric structure which means they have a central tube surrounded by bigger tubes. By the year 1991 it was possible to characterize CNTs sufficiently in order to validate the discovery of new form of carbon [14]. Since 1991 the number of scientific publications related to CNTs has been increasing almost exponentially [15].

2.3. Properties of CNTs

2.3.1. Mechanical

In CNTs, carbon atoms are bonded with π-bonds which are very strong bonds. This is the reason for their ultimate strength and stiffness. Depending on the number of sidewalls and defects, CNTs can have different Young's modulus. For example, the highest of Young's modulus is about 1 TPa if the tube is 1- 2 nm in diameter, smaller tubes are mechanically instable and larger tubes are approaching graphite [17]. It must be also noted that this strength comes at low weight, making CNTs desirable for applications that require strength and lightness. Due to their outstanding mechanical properties, CNTs, similarly to carbon fibers, can be used in composite materials to enhance mechanical performance, for e.g., lightweight and strong bicycle parts, tennis racquets and abrasion resisting coatings [16]. Comparison of different CNTs Young's modulus, tensile strength and density to steel is presented in Table 1 [17].

Table 1. Mechanical properties of nanotubes compared to graphite and steel [17].

	Young's modulus (GPa)	**Tensile strength (GPa)**	**Density (g/cm3)**
MWCNT	1200	~150	2.6
SWCNT	1054	75	1.3
SWCNT bundle	563	150	1.3
Graphite	350	2,5	2.6
Steel	208	0,4	7.8

When characterizing CNTs, their remarkable specific surface area cannot be overlooked. Small diameter and high lengths means that very much of their surface is exposed; giving them a specific surface area of up to 1300 m^2/g. The specific surface area (SSA) is dependent on the number of sidewalls. High SSA makes CNTs suitable for applications such as water and air filtering [18, 19 and 20].

2.3.2. Electrical

Due to their graphite structure, CNTs are excellent electrical conductors and can also exhibit semiconducting properties. This phenomenon is caused by chirality which means the direction of graphene sheets are rolled into tubes (Figure 1) [21].

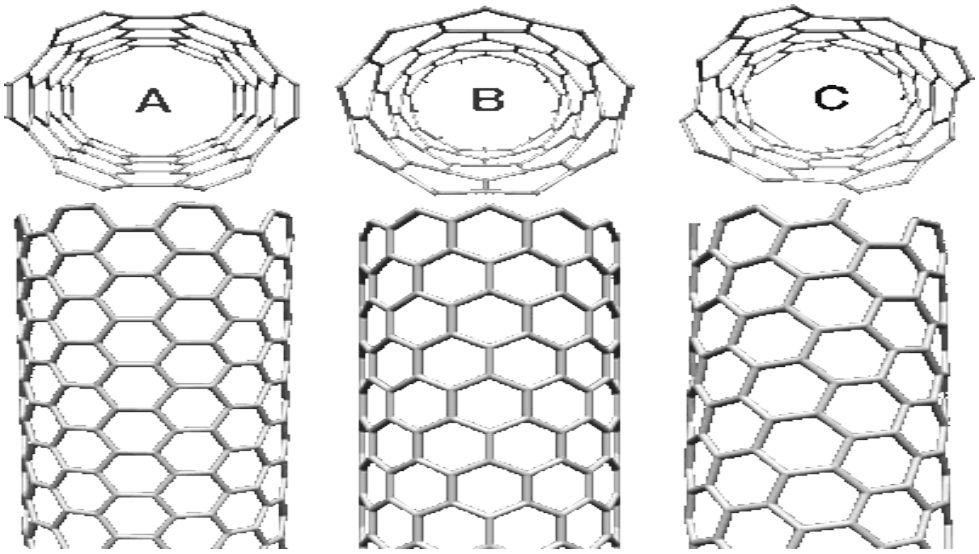

Figure 1. Chirality of CNTs. A) armchair, B) zig – zag, C) chiral [21]

In armchair configuration, the CNTs have metallic properties and are very conducting. This is due to zero band gap, and then electrons can freely move between the conduction and valance bands. However, in zig – zag and chiral configuration, the CNTs are semiconducting. These properties make CNTs particularly attractive for the electronic industry where they can be incorporated to the structure of traditional electronic devices to improve performance or be used for entirely new carbon – based electronics. Possible applications include gas sensors, field emitters, transistors, supercapacitors, conductive plastics, energy storage [22] and electrical cables [23].

2.3.3. Optical

CNTs absorb light in visible to near infrared part of the spectrum. The absorption spectrum reflects information about the structure. By studying the optical absorption spectrum, properties like chirality, diameter [24] and purity [25] of the tubes can be determined. Spectral analysis is a non-destructive method.

In Figure 1 the optical absorption spectrum of CNTs is illustrated. The X-axis corresponds to photon energy and the Y- axis corresponds to the absorbance intensity. The absorbance spectra of CNTs present Van Hove singularities, on Figure 1, marked as S_{11}, S_{22} and M_{11}.

Van Hove singularities are absorption bands as a result of the transitions between valance band and conduction band of CNTs. Based on these transitions, the semiconducting or metallic nature and the chirality of nanotubes can be identified [24]. On Figure 1, distinct peaks S_{11} and S_{22} can be observed, indicating transitions of semiconducting nature. A shallow peak M_{11} shows the presence of metallic CNTs, however as it is low, the semiconducting properties prevail in the given sample. On Figure 2, possible transitions in the nanotube structure are illustrated.

The purity of the material is also characterized by the height of the π-plasmon peak. A low and featureless peak indicates less carbonaceous impurities in the sample [25].

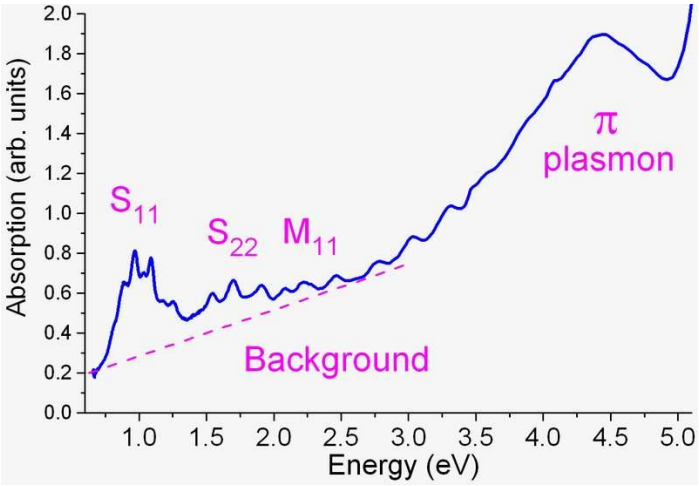

Figure 2. Absorption spectrum of SWCNTs. [26]

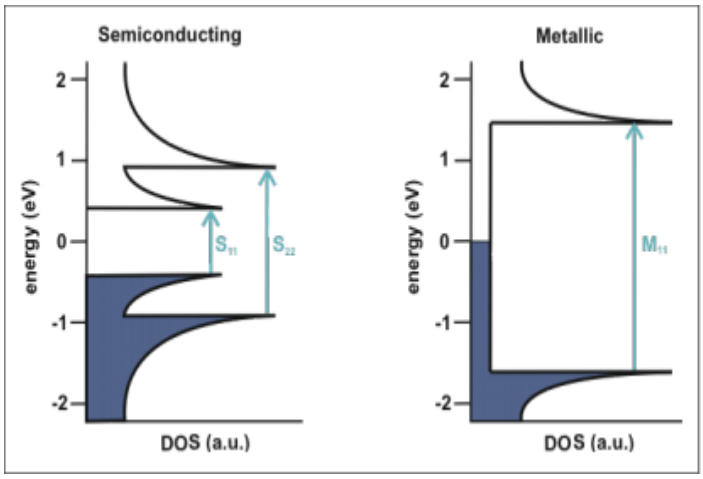

Figure 3. Possible transitions in CNTs [25].

CNTs can be divided into 2 groups: SWNTs and MWCNTs. SWNTs can be semiconducting and metallic. However, MWCNTs are always metallic in nature. It is very difficult to determine the chirality, diameter and purity of MWCNT due to the various graphene layers present and the large number of defects they harbor. In case of metallic nanotubes there is no band gap and therefore optical transitions are not possible. In our case the nanotubes do not contribute optically to the photovoltaic effect but rather serve as conduction pathways for evacuation of charges created by the surface states of HfO_2 and the generation of a photocurrent.

2.4. Functionalization of CNTs

In order to bond CNTs with other materials, they often need to be functionalized to introduce defects on the surface of the CNTs. CNTs are chemically quite inert but defects can improve their chemical reactivity and solubility [27].

Functionalization of CNTs can be divided into chemical and physical methods. In chemical functionalization CNTs are commonly subjected to harsh chemical treatment with strong acids such as HNO_2 and H_2SO_4 or a mixture of them, or strong oxidative chemicals like $KMnO_4$ and O_3. Chemical methods, however, severely damage the sidewalls and thus can affect the properties of the CNTs [27].

Physical methods of functionalizing CNTs employ surfactants and aromatic compounds [27]. In the current thesis CNTs are functionalized by ultrasonication treatment, which also

introduces defects to the sidewalls. Ultrasonication and its effects on CNTs will be further described in the results section of this thesis.

2.4.1. Defects of CNTs

Defect sites serve as functionalities to which other molecules can adhere. Defects in CNTs can be observed as damages to the lattice of graphene. These damages are bends in the CNTs, waviness of the walls and C dangling carbon bonds. Amorphous carbon can also be present on the surface but contrary to aforementioned defects, amorphous carbon is undesired as it contributes to inert properties. Common defects are graphene lattice deformations, atom vacancies and interstitial atoms [28]. Different morphologies of CNTs can also be viewed as defects. Certain morphologies inherently produce deformations in the sidewalls and in the graphene lattice. CNTs can be bent, coiled or have a Y-shaped branched structure. These structural deformations cause the formation of pentagon, heptagon and octagon patterns in the graphene lattice, instead of a hexagon [29].

2.4.2. Toxicity of CNTs

As described previously, CNTs are already used in a number of applications. With this arises the question whether they are safe for human biology. Due to their nanoscale dimensions, CNTs can affect the molecules and cell structures in the human body [30]. A number of studies have been carried out to study the toxicity of CNTs toward human health. The results are still contradictory and consensus has not yet been reached [31, 32].

3. Metal oxide nanoparticles

Metal oxides are an important class of material in materials science due to their wide range of chemical and physical properties and their structure. Metal oxides can exhibit metal, semiconducting or insulating properties and these properties make them promising for electronic applications. Moreover, metal oxides can also be applied as catalysts, corrosion protection coatings and fuel cells [33, 34].

3.1. Metal oxide nanoparticles production methods

3.1.1. Mechanical

Nanoparticles are produced mechanically by ball milling method, usually used in industry for producing fine powders like cement and clay. When scaled down and refined, it can also be applied for nanoparticle production. Ball milling is a top-down synthesis technique.

A ball mill is a simple device, comprising of a revolving drum and high strength metal balls in the drum that move freely. In ball milling a powder mixture of a desired substance is subjected to high energy collisions. Disadvantage of this method is low level control over size distribution of the particles produced [35, 36]. Scheme of a ball mill is shown on Figure 4.

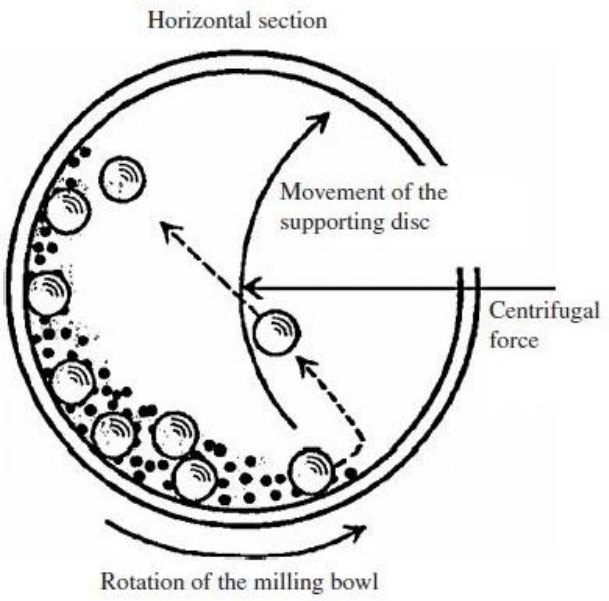

Figure 4. Scheme of a ball mill [35].

3.1.2. Hydrothermal synthesis

Hydrothermal synthesis is generally defined as crystal synthesis or crystal growth under high temperature and high pressure water conditions from substances which are insoluble in ordinary temperature and pressure (100°C, 1 atm). In hydrothermal method, water is taken to supercritical condition, meaning above its boiling temperature and atmospheric pressure.

The solvent properties of water are dependent on pressure and temperature and tuning these values enables to achieve specific solvent properties. This also offers control over precursor solving and crystal formation [37].

The precursors used in the synthesis of inorganic particles are usually aqueous solutions of simple salts like metal chlorides, nitrates or acetates. Depending on the specific synthesis, additives and surfactants can be added prior to the process for the improvement and control of the particle properties [38].

3.1.3. Non – aqueous sol – gel

In non-aqueous sol-gel chemistry the transformation of the precursor takes place in an organic solvent without water. Non-aqueous sol-gel chemistry enables to use wider variety of precursors compared to aqueous sol-gel. List of possible precursors also include inorganic metal salts, metal acetates and metal alkoxides [39]. The reactions occur at relatively high temperatures (200 – 300^{o}C) and generally, the presence of surfactants and coordinating solvents is necessary to stabilize and control the particle growth. Also, capping agents may be used, that offer control over the surface properties of NPs and prevent agglomeration. Via non-aqueous sol-gel many metal oxide nanoparticles can be synthesized, the list includes TiO_2, SnO, FeO_X, CrO, CoO, NiO, ZnO, HfO_2 and many more [40].

3.2. Health concerns, toxicity

Due to rapid development of nanotechnology and increasing production of metal oxide nanoparticles, humans are more likely to be exposed to nanoparticles via commercial products or occupationally. For example, metal oxide NPs are already used in sunscreens, toothpastes, electronics and medicine. Toxicity studies of metal oxide nanoparticles are not very numerous. Furthermore, due to increasing demand and production of different nanoparticles, conclusive data about their toxicity is limited. However, a few studies in which cytotoxicity of different metal oxide nanoparticles is studied have been carried out [41, 42]. It was found that virtually all metal oxide nanoparticles observed (CuO, TiO_2, ZnO, Fe_3O_4, Fe_2O_3, Al_2O_3, and CrO_3) exhibit cytotoxicity towards mammalian cells, the most potent being CuO. In comparison, TiO_2 was the least toxic.

As hafnium is located in the same group as titanium in the periodic table, it can be speculated that HfO_2 nanoparticles are also of low cytotoxicity. This speculation is supported by a publication [43] in which the cytotoxic properties of HfO_2 nanoparticles were tested on living cells. The results revealed that Hf imposes low to mild toxicity even in high concentrations. The literature provides only a few papers concerning the toxicity of hafnium compounds towards living cell. Moreover, to the best of my knowledge, the aforementioned reference is the only one concerning the toxic effects of specifically HfO_2 nanoparticles.

4. CNT/metal oxide nanoparticle based hybrid structures

4.1. Morphological characterization of hybrid materials via TEM

Studying the topology of CNT/metal oxide nanoparticle based structures offers a comparison between the material synthesized during this master's project and other similar hybrid materials. Based on the topological characteristics of other well performing and possibly already applied nanohybrid structures, conclusions can be drawn as to what kind of improvements CNT – HfO_2 nanohybrid still might need in further research.

Based on the literature, by far the most studied CNT/metal oxide nanoparticle hybrid structures are accordingly CNT/TiO_2 and CNT/ZnO. In this chapter, the topology of these hybrids will be reviewed.

The interest in TiO_2 nanoparticles is their photocatalytic activity and ability to decompose various pollutants under UV light. However, useful properties of TiO_2 are not limited to photocatalysis. TiO_2 NPs are promising for renewable energy solutions, sensors and solar cell technologies as well. CNTs serve the role of nanoparticle support material in the composite [44].

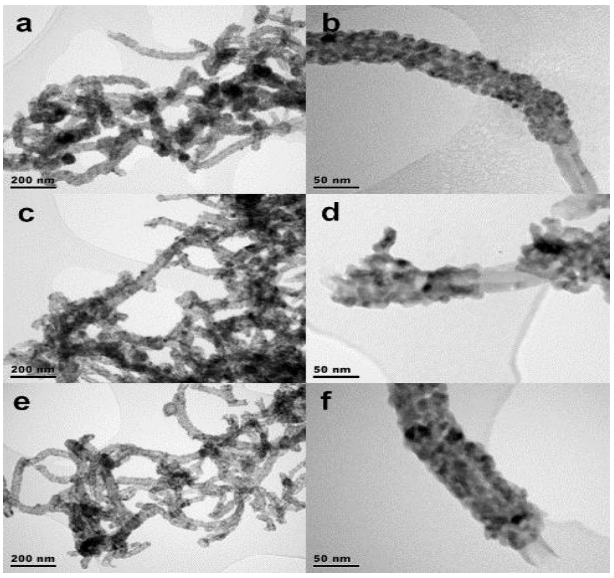

Figure 5. TEM images of calcinated CNT/TiO_2 nanocomposites prepared from pristine CNTs with different TiO2 precursors: (a and b) titanium isopropoxide; (c and d) titanium butoxide; (e and f) titanium ethoxide. Images on right hand side show comparisons in thickness of TiO_2 layer [45].

In Figure 5, TEM images provide an overview of CNTs decorated with TiO_2 NPs produced from different precursors. The images show very uniformly decorated CNTs and small area of uncovered CNTs. The nanoparticles are covering large area of each individual nanotube and show very low degree of agglomeration, making for efficient coverage. The reference article also describes the effects of different TiO_2 layer thickness on photocatalytic and photoelectrocatalytic properties of the nanohybrid [45].

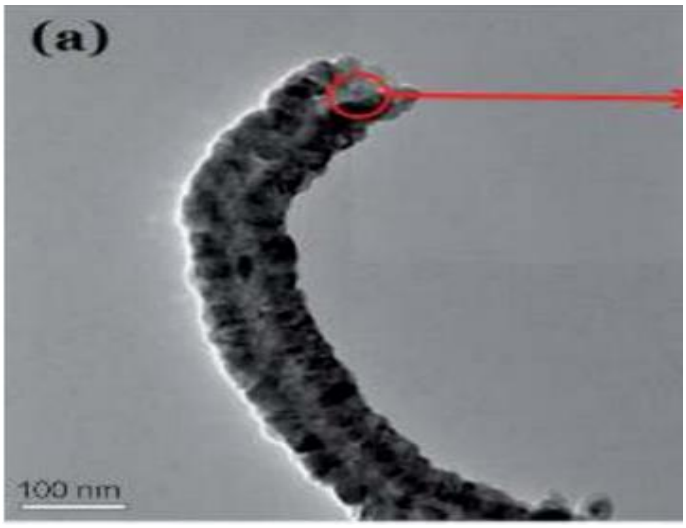

Figure 6. HRTEM image of a CNT coated in ZnO nanoparticles [46]

ZnO, like TiO_2, exhibit properties applicable in photovoltaics. In addition ZnO also emits light in visible and UV range of spectrum. Taking this into account, it is comparable to the nanohybrid that is under observation in this thesis. Figure 6(a) shows a carbon nanotube coated with ZnO nanoparticles. Coverage is uniform and anchoring of the NPs seems not governed by the defects in CNTs.

5. THE OBJECTIVES AND METHODOLOGY

The objective of the current thesis is to study the functionalization of CNTs by ultrasonication and the properties of new nanohybrids composited of MWCNTs and HfO_2 nanoparticles. This masters thesis was conducted in the frame of collaboration with Dr. Protima Rauwel from University of Tartu who initiated this project. It is expected that these new nanohybrids will demonstrate properties that both components do not show individually. The plan was to study the influence of the synthesis process and determine the optimal growth parameters in a future study. This research project was carried out with the collaboration of Minatec LAHC in Grenoble France via a PARROT project between Estonia and France. This collaboration included experiments to investigate the electrical-photogalvanic properties and AFM measurements to study the surface topography of the material. These studies were carried out in collaboration Dr. Frederique Ducroquet and Dr. Irina Ionica, respectively. The outcomes of these experiments will be presented in results and discussion section.

To achieve the objectives, methodology consists of the following tasks:

1. Synthesis of HfO_2 nanoparticles
2. Research of CNTs and metal oxide nanoparticles and their interfaces
3. Synthesis of the MWCNTs – HfO_2 nanohybrid via sonication
4. TEM studies of the synthesized nanohybrid
5. Sonication effects on dispersion of the CNTs
6. Sonication effects on the dispersion and agglomeration of HfO_2 nanoparticles
7. Defects in CNTs induced by sonication
8. Electrical and photocurrent measurements of different sonication time material samples

6. EXPERIMENTAL

6.1. HfO_2 nanoparticles synthesis and characterization

6.1.1. Synthesis of HfO_2 nanoparticles

The procedure for synthesizing HfO_2 NPs was carried out in a glove box (O_2 and H_2O<1 ppm). In a typical synthesis, hafnium tert-butoxide ($(Hf(OtBu)_4$) precursor (STREM 99.9%) (0.87 mmol) was added to 20 ml (183 mmol) of benzylamine (purified by redistillation (99.5%), Aldrich). The reaction mixture was transferred into a stainless steel autoclave and carefully sealed. Thereafter, the autoclave was taken out of the glove box and heated in a furnace at 300˚C for 2 days. The resulting milky suspensions were centrifuged; the precipitates were thoroughly washed with ethanol and dichloromethane; and subsequently dried in air at 60˚C [47].

6.2. HfO_2 nanoparticles characterization

HfO_2 nanoparticles were fully characterized before the start of this study. The structural characterizations of these HfO_2 nanoparticles will be described in this part, but these results were not obtained during this research project.

6.2.1. X-ray diffraction, XRD

X-ray diffraction is the method of projecting a beam of x-ray radiation at a target object and through to a photographic film on the far side. A series of spots appear on the photographic film following this exposure, which is formed by the x-ray radiation diffracting off the structure that they passed through. These diffraction patterns give an indication of the general structure of the object. X-ray beam is diffracting orbiting electrons that are close enough to the core (nucleus) of the atom to give a good indication of the structure of the unit cell [48].

XRD patterns were obtained using Bruker D5000 XRD instrument equipped with a Braun position sensitive detector, both using Cu K_α radiation. The analysis of the XRD pattern in Figure 7 illustrates that the HfO_2 nanoparticles possess the cubic crystal structure (Fm-3m) with a = 0.509 nm [49].

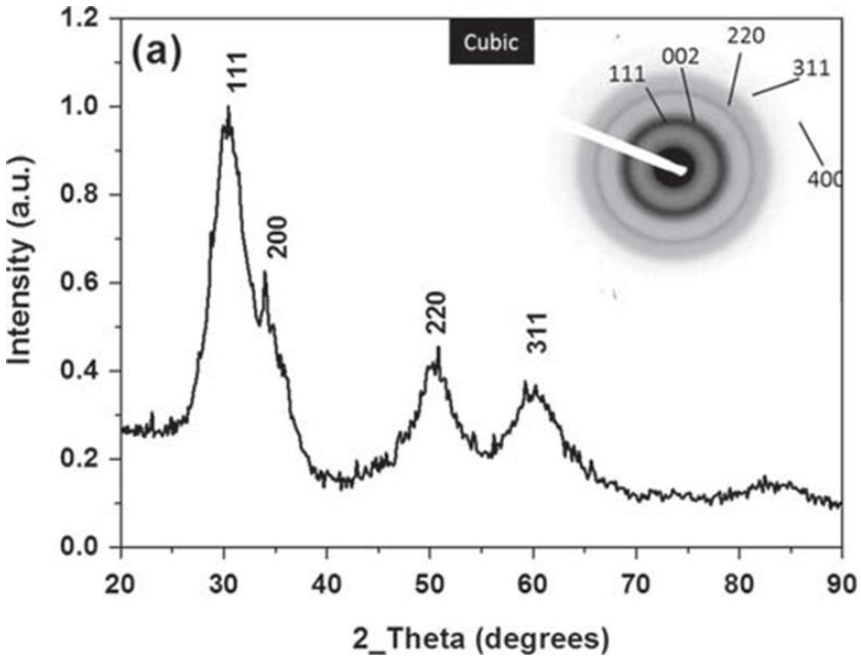

Figure 7. XRD patterns of (a) cubic HfO_2 nanoparticles, inset: Selected area electron diffraction (SAED) pattern of HfO_2 cubic nanoparticles [49].

6.2.2. HRTEM

High resolution transmission electron microscopy (HRTEM) was carried out on a G2 80–200 FEI Titan, operating at 200 kV, disposing a point to point resolution of 0.9 Å. The point to point resolution in TEM mode is 2.4 Å. HRTEM (High Resolution Transmission Electron Microscopy) is an imaging mode of TEM for high magnification studies of nanomaterials. High resolution enables it to image materials on the atomic scale. Traditional microscopy is limited to the optical diffraction limit [50] whereas HRTEM is only limited by the wavelength of electrons that is dependent on the acceleration voltage of the electrons. Wavelength of electrons is 0.0027 nm when applying 200 kV [51].

TEM works by extracting electrons from an emitter and focusing them with the help of electromagnetic lenses before allowing them to be transmitted by a specimen. The image is a pattern of electrons that have interacted with the specimen. Image formation process in TEM is illustrated on Figure 8.

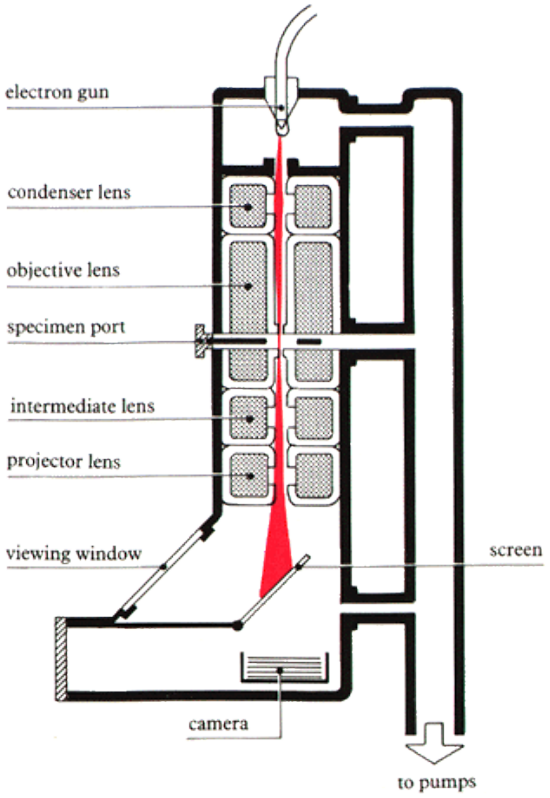

Figure 8. Image formation in a transmission electron microscope [52].

6.3. MWCNT – HfO_2 nanohybrid synthesis

6.3.1. Materials

In the experiment Nanocyl^{TM} NC7000 series MWCNTs were used. NC7000 nanotubes have an average diameter of 9.5 nm and average length 1.5 microns. Surface area of given nanotubes is 250-300 m^2/g. Purity of CNTs is 90%, metal (catalyst) residues make up 10%. NanocylTM NC7000 nanotubes are produced via chemical carbon deposition process (CCVD). Amorphous carbon on the walls of nanotubes can be expected due to the CCVD production process itself [53].

Formation of MWCNTs during CCVD process takes place as gaseous hydrocarbons are passed through a tubular reactor in the presence of a catalyst material at high temperature (600 – 1200^{o}C). High temperature decomposes the hydrocarbon and catalyst serves as nucleation center onto which CNTs will grow. CNTs are collected once the reactor is brought down to room temperature. This process also enables to use hydrocarbons in liquid and solid

state as the CNTs precursor material. Although CVD method is commonly agreed to be reasonable in terms of production cost and quantity, it still yields nanotubes with some metal impurities [54]. Depending on the producer, CNTs may contain metal elements (Fe, Ni, Mo, Co) contaminants 1-10% [55]. The synthesis and structural characterization of the cubic HfO_2 nanoparticles with an average diameter of 2.5 nm used in this study was described previously.

6.3.2. Methods and apparatus

12 mg of MWCNTs and 12 mg of cubic HfO_2 nanoparticles were measured using a lab scale (Precisa XT120A). Then, the materials were rinsed out of the tubes with ethanol and mixed together in a bigger tube containing 15 ml of pure ethanol.

Firstly, the solution was mixed by manually shaking the tube for 2 minutes without any sonication treatment, and a control sample of 1.5 ml was taken from the primary solution and the tube containing the remaining 13.5 ml of solution was then introduced into an ultrasonic bath for mixing. A sample of 1.5 ml of the solution was collected every 30 minutes over a total period of 3 hours.

For sonication, an ultrasonic bath (Bandelin sonorex digitec) was used. The temperature of the bath was set for 40^{o}C. Due to excessive heat generation by ultrasonic in aqueous media, the water was changed regularly every 30 minutes to prevent the ethanol from evaporating.

6.4. HfO_2 nanoparticle - ethanol solution concentration

It is important to calculate the concentration of cubic HfO_2 NPs in the prepared solution in order to tune this concentration for future studies.

XRD study showed the crystal structure of the HfO_2 NPs is a face–centered-cubic lattice (FCC) and HRTEM study showed that the average diameter of the HfO_2 NPs is 2.5 nm. With this information it is possible to calculate the concentration of HfO_2 nanoparticles present in the nanohybrid composite.

First of all, it is necessary to determine the number of Hf and O atoms in one unit cell. In HfO_2 cubic unit cell, every hafnium atom is bonded to 8 oxygen atoms and every oxygen atoms are bonded to 4 hafnium atoms. Hafnium atoms are located in the corners and in the center of the faces of the cubic unit cell, whereas the oxygen atoms occupy the 8 tetragonal

sites inside the cube (see Figure 9). As the cubic structure has six faces and for each a half atoms in the unit cell, these are multiplied and added to the eight corner atoms.

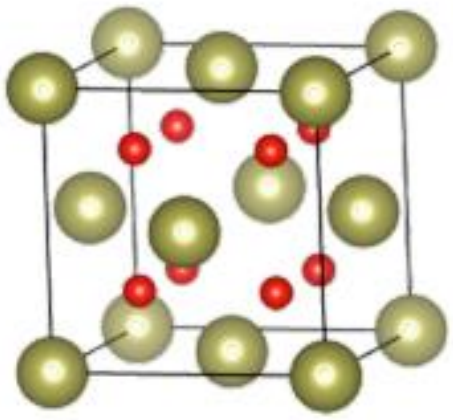

Figure 9. Representation of HfO_2 cubic unit cell structure [56]

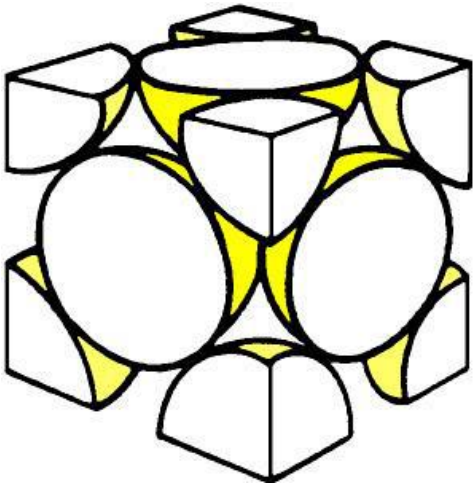

Figure 9. Structure of face centered cubic unit cell for calculations [57]

$$Z_a = \frac{1}{2}f + \frac{1}{8}c \qquad \text{(Eq. 1)}$$

Where: Z_a – number of Hf atoms in the unit cell

f – number of faces in unit cell

c – number of corners in unit cell

Each unit cell contains 4Hf atoms and 8 O atoms.

The length of the cubic unit cell has been calculated in an earlier publication [49] and is 5.09 Å. The volume of the unit cell is calculated as the volume of a cube.

$$V_{uc} = a^3 \quad \text{(Eq. 2)}$$

Where: V_{uc} – volume of unit cell

a – length of the side of cubic unit cell

HfO_2 nanoparticles are spherical with a diameter of 2.5 nm, therefore the volume of a nanoparticle is calculated using the formula of volume for a sphere.

$$V_{NP} = \frac{4}{3}\pi r^3 \quad \text{(Eq. 3)}$$

Where: V_{NP} – volume of a nanoparticle

r – radius of a nanoparticle.

Once the volume of a unit cell and the volume of a nanoparticle is calculated, the number of unit cells in a nanoparticle can be found.

$$Z_{uc} = \frac{V_{NP}}{V_{uc}} \quad \text{(Eq. 4)}$$

Where: Z_{uc} – number of unit cells

V_{NP} – volume of nanoparticle

V_{uc} – volume of unit cell.

Once we know the number of unit cells in one nanoparticle, we can calculate the molecular weight of one HfO_2 nanoparticle.

$$M_{HfO_2NP} = Z_{uc} \times (4M_{Hf} + 8M_o) \quad \text{(Eq. 5)}$$

Where: M_{HfO2NP} – molecular weight of one HfO_2 nanoparticle

M_{Hf} – molecular weight of hafnium

M_O – molecular weight of oxygen

Z_{uc} – number of HfO_2 unit cells in one nanoparticle

To find the amount of HfO_2 in moles, we need to divide the mass of the used HfO_2 by the molecular weight of one HfO_2 nanoparticle.

$$\frac{m_{HfO_2}}{M_{HfO_2}} = moles\ of\ HfO_2 \quad \text{(Eq. 6)}$$

Where: M_{HfO2} – molecular weight of one HfO_2 nanoparticle

m_{HfO2} – mass of HfO_2

For NP concentration in the ethanol solution, we divide the number of mole we calculated by the volume of ethanol.

$$\frac{moles\ of\ HfO_2}{V_{ethanol}} = NPs\ concentration \quad \text{(Eq. 7)}$$

Thermogravimetric analyses (TGA) showed that in the case of cubic HfO_2, a total weight loss of about 14% is estimated up to 800˚C, speaking for the organic species adsorbed on

the surface of the nanoparticles. This part of organic species has to be taken into account for the calculation of the concentration of HfO_2 nanoparticles in the solution. 12 mg of HfO_2 nanoparticles contains 1.68 mg of organic species and then contain 10.32 mg of HfO_2 nanoparticles.

6.5. Surface area of CNTs

In order to find the nanoparticle coverage of the CNTs, the surface area of nanotubes must be calculated as well. Nanocyl NC7000 multi-walled carbon nanotubes datasheet [53] indicates a specific surface area of 250-300 m^2/g and a purity of 90%. The amount of CNTs introduced in the solution was 12 mg, which means that the real weight of MWCNTs is 10.8 mg.

To find the surface area, the weight of the introduced MWCNTs must be multiplied by SSA given on the datasheet.

$$S = S_{SSA} \times m \qquad \text{(Eq. 8)}$$

Where: S – surface area

S_{SSA} – specific surface area

m – weight of CNTs

6.6. Nanoparticle coverage of the CNT surface

To find the optimum balance of nanoparticles and CNTs in the solution, the total area of CNTs covered by nanoparticles must be calculated. The aim was to cover approximately 10% of the CNT surface.

First, the area that nanoparticles can possibly cover theoretically has to be calculated. For this we will find the cross – sectional area of a single nanoparticle and then multiply it by the total number of nanoparticles in the solution, which was calculated previously. Since HRTEM study showed that the cubic HfO_2 nanoparticles are spherical, we can use the formula of circle area for the calculation.

$$S_{NPCS} = \pi r^2 \qquad \text{(Eq. 9)}$$

Where: S_{NPCS} – cross-section area of one nanoparticle

r – radius of one nanoparticle

And the total cross-section area of NPs.

$$S_{NPCS} \times number\ of\ NPs = total\ NP\ covered\ area \quad \text{(Eq. 10)}$$

Where: S_{NPCS} - cross-section area of one nanoparticles

Next step is to divide the total cross-section surface area of used NPs by the surface area of CNTs.

$$S_C = \frac{total\ NP\ covered\ area}{S} \quad \text{(Eq. 11)}$$

Where: S_C – surface covered

S – surface area of CNTs

6.7. Atomic force microscopy, topology of the nanohybrid

Atomic force microscopy (AFM) was carried out at Minatec LAHC in Grenoble, France, under the supervision of Dr. Irinia Ionica. AFM was done to study the topology of CNT - HfO_2 nanohybrid.

Atomic force microscopy works by "dragging" the probe across the surface of the material and interpreting the forces between the probe and surface. Laser beam is targeted at the cantilever and is deflected as the cantilever follows the topology of the sample. The deflections are converted into an image of the surface. Simplified scheme of AFM working principle is illustrated on Figure 10.

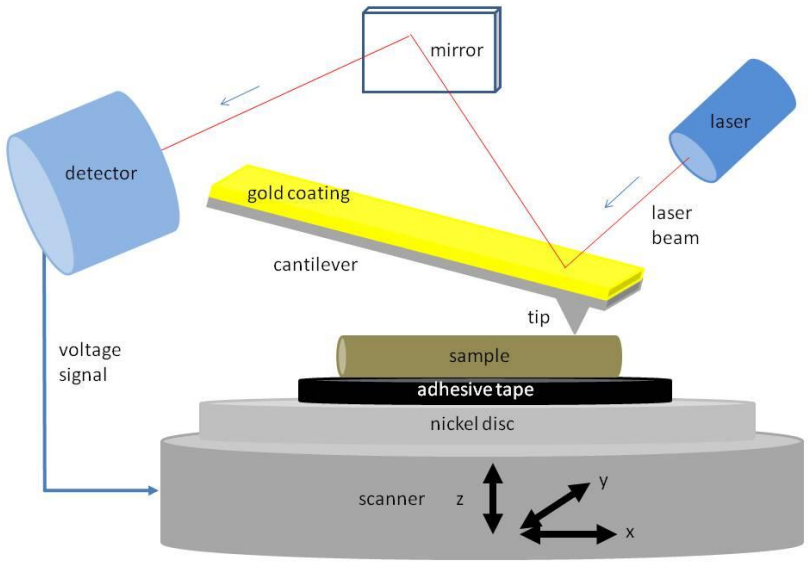

Figure 10. The working principle of atomic force microscopy [58].

6.7.1. AFM sample preparation

For AFM studies four samples were prepared on different supports. Two samples on a glass support and the others on a ceramic support with a metal contact. In both cases, the material sample sonicated for 180 minutes was used. A droplet of the material solution was deposited on the glass support with a pipette. Once the ethanol had evaporated, a thin copper wire was attached to the sample for polarizing it in the AFM. Samples on the ceramic supports were prepared the same way, but the copper wire was soldered onto the metal contact.

6.7.2. Apparatus

Nanoscope IV atomic force microscope was used for topological study of the nanohybrid samples. This method and apparatus provide a resolution down to 1 nm. AFM was used in TUNA mode (tunneling AFM) that also enables to measure and characterize currents in the range of 1 pA.

6.8. Electrical measurements

Electrical measurements were carried out under the supervision of Dr. Frédérique Ducroquet. Samples were prepared and their conductivity, photocurrent and photo capacitance were measured.

6.8.1. Conductivity and photocurrent sample preparation

For sample preparation ceramic supports with metal contacts were used. Supports measured 1.5 cm by 2 cm and had 12 metal contacts which were 1 mm apart (Figure 11). Samples were deposited between the metal contacts using a pipette. Samples were as follows: pure CNTs, 0 min, 30 min, 60 min, 90 min, 120 min, 150 min and 180 minutes of sonication time accordingly.

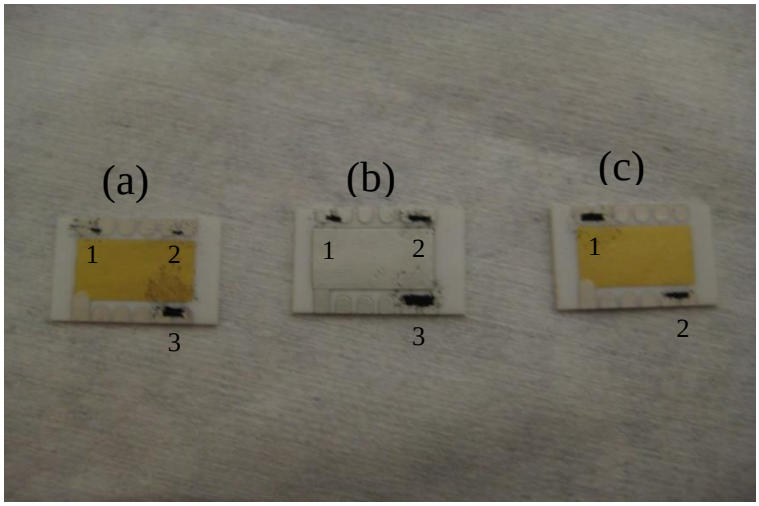

Figure 11. Samples for conductivity and photocurrent measurements. Support (a): 1 - pure CNTs, 2 – 0 min, 3 – 30 min. Support(b): 1 – 60 min, 2 – 90 min, 3 – 120 min. Support(c): 1 – 150 min, 2 – 180 min.

6.8.2. Photocapacitance sample preparation

Samples were deposited on the metal pad of a ceramic support by using a pipette. When the ethanol had evaporated, the samples were covered with UV – invisible resin (Figure 12) and placed to set under a powerful UV lamp to harden. Then a drop of silver paste was applied on the resin to achieve good contact for measuring equipment.

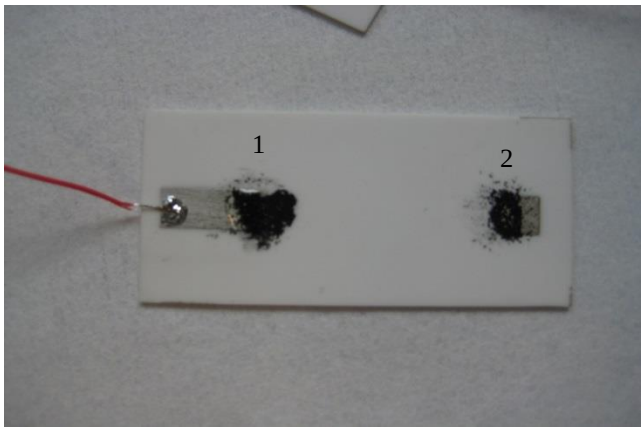

Figure 12. Capacitor sample, on the right covered with UV invisible resin. On the right 180 min sample (1), on the left pure CNTs (2).

6.8.3. Apparatus and methods

Photocurrent, IV, dV measurements were carried out using a Hewlett – Packard 4155A Semiconductor Parameter Analyzer. Photo-induced capacitance was measured on Agilent E4980A Precision LCR Meter (20 Hz to 2 MHz). This equipment also included a microscope and precision electrodes. The microscope with electrodes was placed on a granite slab for seismic stability.

For photocurrent measurements, the samples were first tested for conductivity and IV-curves (current and voltage, respectively) were constructed, both in the dark and under illumination by halogen lamp and UV-lamp. IV- curves show conductivity through the sample and helps to determine whether or not there is a contact between the contacts on the support through the material. Halogen light and UV light was used to see if they have an effect on the conductive properties of the material. Moreover, deltaV measurements were done to see photocurrent generation under illumination by halogen and UV.

Table 2 recapitulates the various experiments performed on each samples during the stay in Grenoble.

Table 2. Samples prepared for electrical measurements and atomic force microscopy (VPC – visible photocurrent).

	Sample (sonication time in minutes)								
Purpose	Pure CNTs	0	30	60	90	120	150	180	Support type (quantity)
AFM								X	Glass (2)
								X	Ceramic with metal contacts (2)
Capacitance	X			X		X		X	Ceramic with metal contacts (1)
Electrical, photocurrent	X	X	X	X	X	X	X	X	Ceramic with metal supports (1)
	X	X	X (VPC)	X	X	X			Silicon wafer (1)

7. RESULTS

7.1. TEM studies of MWCNT – HfO_2

0 minutes sonication time

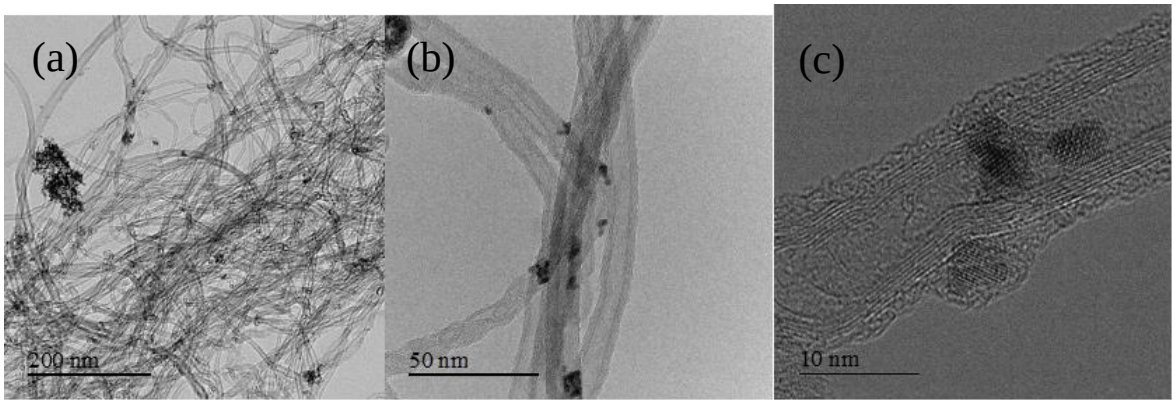

Figure 13. TEM images of manually agitated solution of MWCNTs-HfO_2, (a) overview of material, (b) high magnification image of material, (c) HRTEM image of a CNT

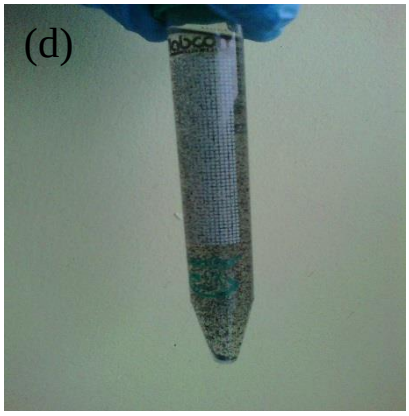

Figure 13. (d) 0 min sonication, manually agitated mixture of CNTs – HfO_2 nanoparticles

TEM images of the material (Figure 13 (a, b) reveal that with no sonication the nanoparticles stick at or near certain bending points of nanotubes. These anchoring points indicate defects in the graphene sheet lattice. From this it can be concluded that CNTs used in this experiment have initially some wall damage. It is also clear that NP dispersion over CNTs is not uniform and is concentrated in certain places. Also, there is a noticeable layer of amorphous carbon on the CNT surface (Figure 13(c)) which complies with the information provided on

NC7000 data sheet. Furthermore, CNTs are clearly bundled implying that the whole CNT surface is not exposed to nanoparticles. Bundling was also observable to the eye when CNTs and HfO_2 NPs were initially mixed together after manual agitation where the hybrid nanomaterial did not disperse uniformly (Fig. 13(d)).

30 minutes sonication time

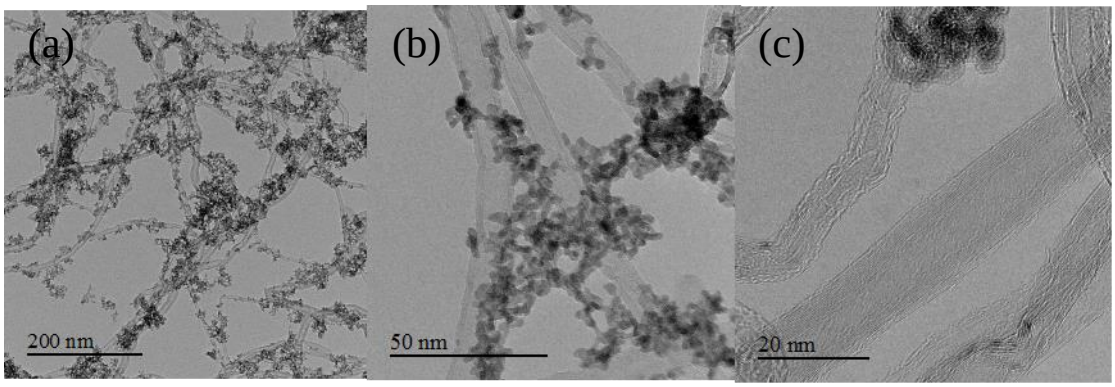

Figure 15. TEM images of MWCNTs-HfO_2 sonicated for 30 minutes, (a) overview of the material, (b) high magnification image, (c) HRTEM image of a CNT

On figure 15(a) drastic changes can be observed. After only 30 minutes in an ultrasonic bath, dispersion of NPs is a lot more homogenous. CNTs are more evenly decorated with nanoparticles (compared to fig. 13(a, b, d)) but agglomeration of particles is still observable. On Figure 15(b) nanoparticle agglomeration can be seen on a smaller scale and it shows agglomerates on CNT sidewalls, which in turn has formed agglomerate, this time along with CNTs. This is not desired and more sonication is needed. An earlier study showed that sonication can be used to fragment nanoparticle clusters in the case of ZnO [59], Al_2O_3 [60] and TiO_2 [61] but for HfO_2 particles, this has not been studied before. The bundling effect of CNTs has reduced compared to Figure 1(a) with 0 min sonication time. Another change is that CNT surface has much less amorphous carbon after 30 mins sonication (Fig. 15(c)). This is probably caused by sonication as it also tends to remove amorphous carbon from the surface of the CNTs [62]. It is reported that in the mixture of CNTs and organic liquids, ultrasound causes hot spots where temperature and pressure may exceed 5000 K and 100 MPa [63, 64] which is more than sufficient to remove amorphous carbon and damage the walls of other tubes that have less amorphous carbon by causing waviness and crimps in the

CNT sidewalls (Fig. 15(c)). Hot spots [63] are caused by cavitation which can be explained as the formation and almost immediate collapse of vapor bubbles in a liquid [65] when it is subjected to rapid changes, in this case, ultrasonic waves passing through the solution. In current case cavitation seems to have caused the elimination of amorphous layer on the tube.

60 minutes sonication time

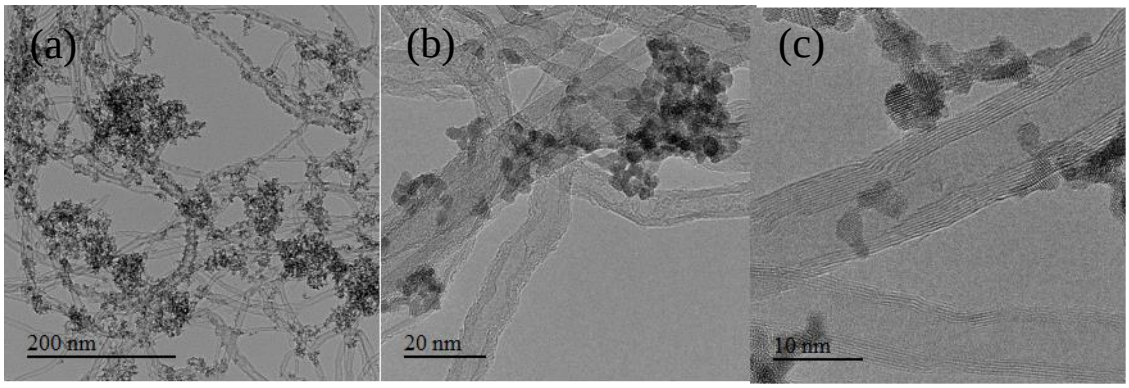

Figure 16. TEM images of MWCNTs-HfO_2 sonicated for 60 minutes, (a) overview of the material, (b) high magnification of the material, (c) HRTEM image of a CNT with nanoparticles.

Compared to Figure 15(a) there is a greater degree of particle agglomeration on Figure 16(a). Agglomeration can be attributed to the high surface energy of nanoparticles [66]. Another factor in particle agglomeration can be high concentration of nanoparticles in the synthesized nanomaterial. On the other hand there are some very uniformly coated nanotubes where particles are attached on the straight sections of the tubes as well and not only on obvious topological defect points. This indicates some additional defects on the otherwise quite inert surface of the tubes. This kind of defect is most likely created by a vacancy, which in turn is likely to have been generated by ultrasonic waves damaging the outer layers of CNTs. Although on Figure 16(b) there are bends in nanotubes, which could possibly provide anchoring sites for nanoparticles, yet they remain undecorated. No clear observable outer layer defects, such as broken sidewalls or amorphous content, can be detected but there is some waviness to them and also a difference in the number of sidewalls between two tubes shown on Fig. 16(c). In addition, Figure 16(c) shows no traces of amorphous carbon on the

sidewalls, however, small quantities of amorphous carbon cannot be neglected, even though not visible in the images.

90 minutes sonication time

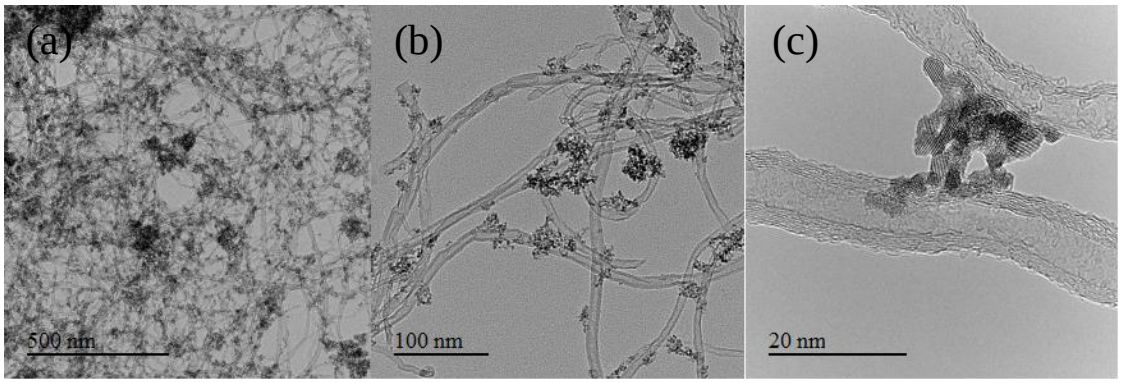

Figure 17. TEM images of MWCNTs-HfO_2 sonicated for 90 minutes. (a) overview of the material, (b) high magnification of the material, (c) HRTEM image of a CNT with nanoparticles

Figure 17(a) shows very nice dispersion of tubes and nanoparticles over them. Overall the sample is very uniform, apart from some moderate agglomeration of nanoparticles, but it has decreased compared to the Fig. 13(a), Fig. 15(a) and Fig. 16(a). On Fig. 17(b), a smaller network of nanotubes with nanoparticles anchored to them can be observed, where tubes are not evenly coated but agglomerates are noticeably smaller in comparison to Fig. 13(a), Fig. 15(a) and Fig. 16(a). On Fig. 17(c) damages to CNT walls are noticeable, not only on outer walls but on the inner walls as well. These damages are observed as waviness to the walls and amorphous carbon in small quantities on outer and inner surface of the CNTs. Amorphous carbon can be attributed to breaking of the C=C bonds on the surface along with some amount of pyrolitic carbon remaining on the walls. It should be however noted that even at 60 minutes sonication hardly and amorphous carbon was visible implying that the most probable origin at 90 min sonication time is C=C bond breaking. This is again likely to be caused by sonication induced cavitation [62, 63, 64, 65].

120 minutes sonication time

(a)

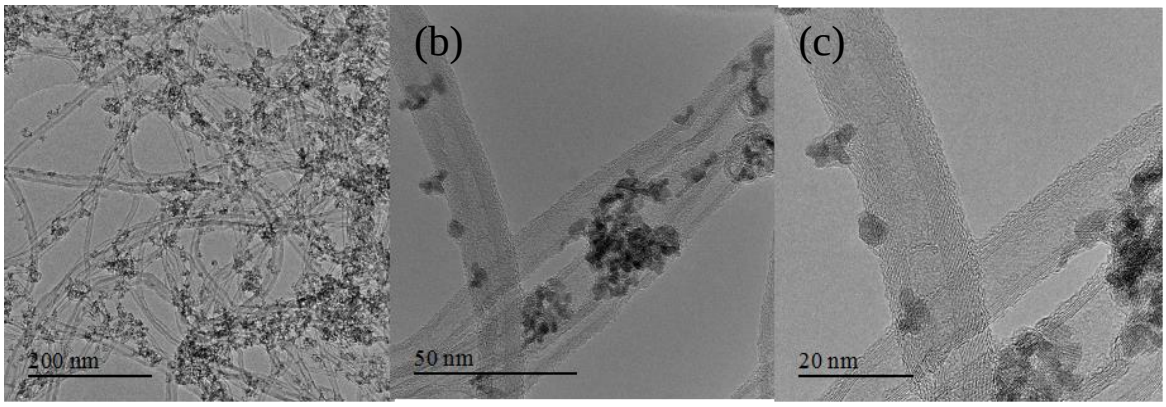

Figure 18. TEM images of MWCNTs-HfO_2 sonicated for 120 minutes, (a) overview of the material, (b) high magnification of the material, (c) HRTEM image of CNTs with nanoparticles.

After 120 minutes of sonication we observe a moderately homogenous network of CNTs coated with NPs (Fig. 18(a)) in very small agglomerates. These are clearly seen on Fig. 18(b).CNT distribution has improved compared to samples which have spent less time in the ultrasonic bath. On the surface of the nanotubes there is a very perceivable layer of amorphous carbon (Fig. 18(c)). This layer is thicker than the layer on 90 min sonicated sample where only small amounts of amorphous carbon were observable. This observation further confirms that sonication introduces damages to the CNT walls (both inner and outer), starting from a few dangling C bonds on the walls and eventually forming a uniform layer of amorphous carbon. An amorphous carbon layer of this thickness and uniformity was previously observed on 0 min sonication sample (Fig.13(c)). On Figures 13, 15, 16 and 17 this process of gradual degradation of the CNT walls can be observed to some extent, primarily on the outer sidewalls. However, it must be kept in mind that the same nanotube cannot be studied in every sample. Therefore, similar nanotubes with similar number of walls were compared in each case. CNT sidewalls, in addition to the amorphous content, exhibit mild waviness along the axis. And on the inner walls, there are signs of wall degradation.

150 minutes sonication time

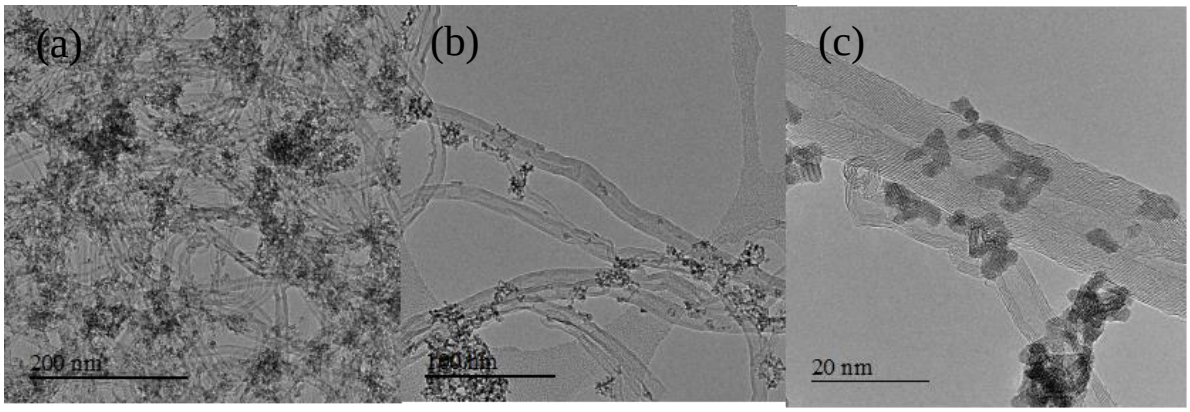

Figure 19. TEM images of MWCNTs-HfO_2 sonicated for 150 minutes, (a) overview of the material, (b) high magnification of the material, (c) HRTEM image of CNTs with nanoparticles

After 150 minutes a very dense network of CNTs with a lot of NPs attached is observable (Fig. 19(a)). Degree of nanoparticle anchoring is very high. Compared to Fig. 15(a) and Fig. 16(a) (comparable scales of 200 nm), a few agglomerates are still present and nanotubes are densely covered in NPs. Figure 19(b) and 19(c) also show good particle distribution along the sidewalls of CNTs. Good anchoring of NPs prove that sonication induces functionalities such as C dangling bonds on the CNT sidewalls. Functionalities also increase solubility of CNTs [67], which in turn makes way for good dispersion. High magnification image (Fig. 19(c)) shows considerable damage to the CNT sidewalls which indicate the start of amorphous carbon formation. Inner walls are damaged too; broken layers of graphene, nanofibers and significant waviness can be seen on Fig.19(c).

180 minutes of sonication

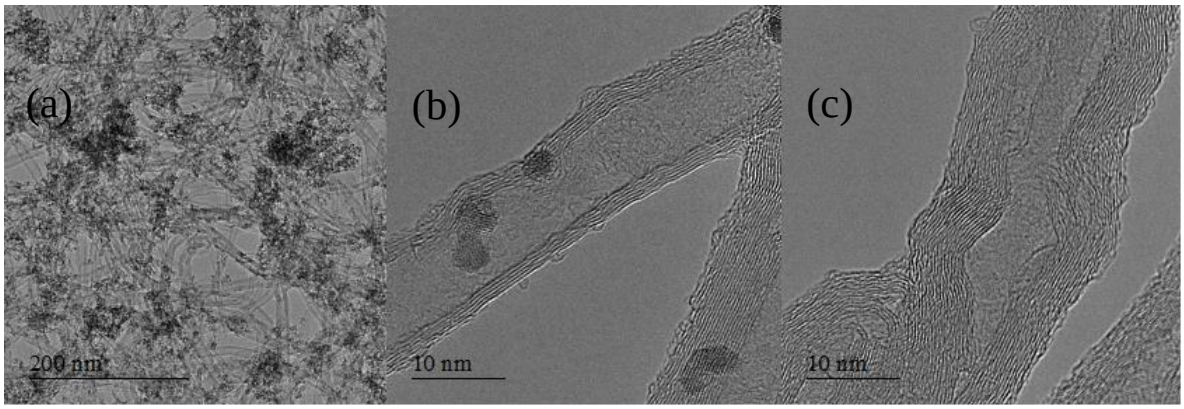

Figure 20. TEM images of MWCNTs-HfO_2 sonicated for 180 minutes. (a) overview of the material, (b) HRTEM image of CNTs with nanoparticles, (c) HRTEM image of CNTs with nanoparticles

After 180 minutes of sonication we obtain a very good dispersion of CNTs and nanoparticles (Fig. 20(a)) which is comparable to previous sample sonicated for 150 minutes (Fig. 19(a)). Overview image shows no significant bundling of CNTs. Figures 20(b, c) show more damage to the CNT sidewalls than Figure 19(c). This illustrates how sonication has further degraded the sidewalls. Similarly to CNTs, sonication has also improved the nanoparticle dispersion. On Fig 20(a), 180 minutes of sonication has dispersed CNTs and nanoparticles and created more function groups on the CNT sidewalls where NPs can anchor. However, there is still some small amount of agglomeration of NPs.

Table 3. Overview of TEM-studied samples.

Sample	Amount (ml)	Sonication time	Dispersion of CNTs/NPs	Anchoring of NPs	Amorphous carbon	Defects of CNTs
MS001	1.5	0	Bundled/agglomerated	Low, big agglomerates	Yes	Bends
MS002	1.5	30	Less bundled/less agglomerated	Good	Very little	Bends, kinks
MS003	1.5	60	Low dispersion/agglomerated	Moderate, some uniformly decorated tubes	No	Bends, wall waviness
MS004	1.5	90	Good dispersion/small agglomerates	Some uniformly decorated tubes	Very little	Wall damage, bends, wall waviness
MS005	1.5	120	Good dispersion/small agglomerates	Good anchoring, some small agglomerates	Yes	Bends
MS006	1.5	150	Very good dispersion/good dispersion with few agglomerates	Good anchoring, some small agglomerates	Little	Bends, kinks
MS007	1.5	180	Very good dispersion/ good dispersion with few agglomeration centers	Good anchoring, some agglomerates	Yes	Wall damage, wall waviness

7.2. HfO_2 nanoparticle - ethanol solution concentration

As described in methodology, it is vital to know the concentration of nanoparticles in the prepared solution of CNTs – HfO_2. This information enables to determine optimal balance between the constituents to achieve optimal concentration of the NPs and therefore, optimal coverage of the nanotubes.

First step, calculating the number of Hf atoms in a FCC unit cell.

$$\frac{1}{2} \times 6 + \frac{1}{8} \times 8 = 4 \quad \text{(Eq. 1)}$$

The oxygen atoms located within the cube structure must also be taken into account. As hafnium atoms are each bonded to eight oxygen atoms and oxygen atoms are each bonded to 4 hafnium atoms we can easily multiply number of Hf atoms by 2, which is 8. This makes a total of 12 atoms, 4 hafnium and 8 oxygen atoms, respectively.

Secondly, the volume of the unit cell is calculated. Volume equals the length of a face to third power. The length of a face of the unit cell is 5.09 Å which is 0.509 nm.

$$0.509^3 = 0.132\ (nm^3) \quad \text{(Eq. 2)}$$

The nanoparticles are spherical; therefore the volume of a single nanoparticle is the volume of a sphere. Average diameter of one HfO_2 nanoparticle is 2.5 nm.

$$\frac{4}{3} \times \pi \left(\frac{5}{4}\right)^3 = 8.18\ (nm^3) \quad \text{(Eq. 3)}$$

The number of unit cells in one nanoparticle.

$$\frac{8.18}{0.132} = 61.9 \quad \text{(Eq. 4)}$$

To find the molecular weight of one nanoparticle, the number of unit cells is multiplied by the sum of molecular weight of the constituents and taking into account the number of Hf and O atoms in the unit cell. There are 12 atoms in one unit cell, 4 Hf and 8 O atoms.

$$61.9 \times (4 \times 178.49 + 8 \times 15.99) = 53796.13 \quad \text{(Eq. 5)}$$

Given that 12 mg of HfO_2 nanoparticle were dispersed in 15 ml of ethanol, we can calculate the concentration of HfO_2 NPs in the solution in μmol/L.

$$\frac{0.01032}{53796.13} = 0.000000192\ (mol) = 0.192(\mu mol) \quad \text{(Eq. 6)}$$

$$\frac{0.192}{0.015} = 12.8\ (\mu mol/L) \quad \text{(Eq. 7)}$$

To find the number of nanoparticles in 10.32 mg of HfO_2, we must multiply the amount of HfO_2 (in moles) by the Avogadro number, which is 6.022 x 10^{23}.

$$1.92 \times 10^{-7} \times 6.022 \times 10^{23} = 1.156 \times 10^{17}\ (number\ of\ NPs) \quad \text{(Eq. 8)}$$

7.3. Surface area of CNTs

In order to find the nanoparticle coverage of the CNTs, the surface area of nanotubes must be calculated. Nanocyl NC7000 MWCNTs datasheet gives the SSA of the used tubes, which is 250 – 300 m^2/g. In calculations we will use the average of 275 g/m^2 and the fact that 12 mg of

CNTs were used. Taking into account that CNTs contain 10% of impurities, the actual weight is 12 mg x 0.9 = 10.8 mg.

To find the surface area, weight of the used CNTs must be multiplied by SSA given on the datasheet.

$$275 \times 0.0108 = 2.97\ (m^2) \quad \text{(Eq. 9)}$$

7.4. Nanoparticle coverage of the CNT surface

To find the optimum balance of nanoparticles and CNTs in the solution, the total area of CNTs covered by nanoparticles must be calculated. The aim was to cover approximately 10% of the CNT surface.

First step is to find the cross – sectional area of a single nanoparticle. Since the HfO_2 nanoparticles are spherical, we can use the formula of circle area for the calculation.

$$\pi \times \left(\frac{5}{4}\right)^2 = 4.91\ (nm^2) \quad \text{(Eq. 10)}$$

Total cross section area of nanoparticles is calculated when cross section area of one NP is multiplied by the number of NPs in 10.32 mg of HfO_2.

$$4.91 \times 1.156 \times 10^{17} = 5.68 \times 10^{17} (nm^2) = 0.568\ (m^2) \quad \text{(Eq. 11)}$$

Next step is to divide the total cross section surface area of used NPs by the surface area of CNTs.

$$\frac{0.568}{2.97} = 0.172 = 19.1\% \quad \text{(Eq. 12)}$$

When evaluating the calculation results, an error bar of 20% should be considered. In the calculations, an average diameter of 2.5 nm was used, but the size distribution diagram shows a size variation from 2 – 3 nm. Due to the method of synthesis that involves the use of benzylamine solvent and no hydrate precursors, the HfO_2 NPs are covered with organic species that is usually called surfactant or stabilizers. The latter aspect was covered based on TGA studies of the NPs that showed an organic content of 14% in mass.

7.5. Electrical measurements

To determine conductive properties of CNTs, current was conducted through the prepared samples and IV-curves were drawn. Voltage from -500 mV to 500 mV was applied on every sample and current up to 10 mA was measured. The IV-curves were linear for all samples tested, showing that CNTs are good electrical conductors. This test was not done with pure CNTs because it proved difficult to achieve contact between the electrodes on the support. The reason for this was poor adhesion between the support and CNTs. In turn, the reason for poor adhesion was the fact that dispersion level of CNTs in ethanol was too high. When the sample was deposited on the support it developed cracks and crumbled after ethanol evaporation.

The photocurrent measurements were first done by illuminating the samples with a halogen lamp and at the same time doing IV curve to see if the light has any effect on the conducing properties. It was expected that the light would excite the nanoparticles and cause charges generation on the surface. HfO_2 nanoparticles are luminescent in pure form, but this was not observed in the nanohybrid. There were some differences between samples under irradiation and samples in the dark, but these effects were inconsistent. Samples were also tested under UV light which also showed no difference in conductance. This was repeated with all the samples that were prepared on ceramic supports, yet none of them yielded the expected results. One assumption was that the CNTs conduction was too high and could mask the possible additional current from the nanoparticles and a higher amount of HfO_2 NPs would be necessary to observe such electrical phenomenon.

dV (potential difference) measurements were also carried out. Similarly to the previous electrical measures, these measurements should have shown a difference in voltage when excited with UV, but no voltage difference was observed. Usually, in such experiment with such low amount of material, a laser is used to excite the sample. However, the laboratory did not have any laser available and the actual UV source was maybe too weak for this experiment.

In order to investigate the generation of charges in the samples, photocapacitance was measured. To give the experiment best possibility of success, the 180 min sonication time sample was selected, as it showed the best dispersion of NPs and CNTs. The samples exhibited capacitance of a few nanofarads in dark. No considerable change in the capacitance value was observed under UV irradiation.

The aforementioned methods of photocurrent measurements were also carried out on the silicon wafer samples. At first these showed no results in the area of interest. But as the silicon wafer is highly reflective a photoluminescent area was clearly observable in a specific area where a higher amount of HfO_2 NPs accumulated on the surface of the silicon substrate (Figure 21). .

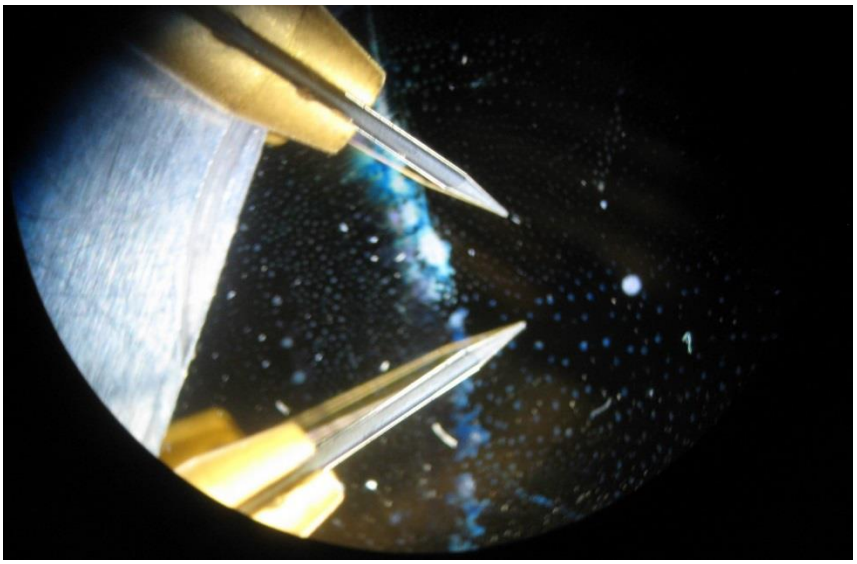

Figure 21. Image of the highly luminous area on a silicon wafer support, photographed trough the eyepiece of the microscope. 30 min sonication time sample.

In a first approach we have measured the current with a polarization of 1mV on this specific area in the dark and under UV excitation. This measurement showed a drop of the current value under UV excitation (Figure 22). The last experiments then concentrated on testing this specific area. I (V) measurements were then performed on this area and the effect of light was clearly visible and reproducible. Figure 23 shows the variation of the current under UV excitation. To confirm that this result is not an artifact, an area of clean silicon substrate and an area of the sample that does not show visible luminescence were also tested. The clean silicon substrate's area did not show any variation under UV excitation and the previous result observed on the luminescent area could then not be attributed to the silicon substrate used as support (Figure 24).

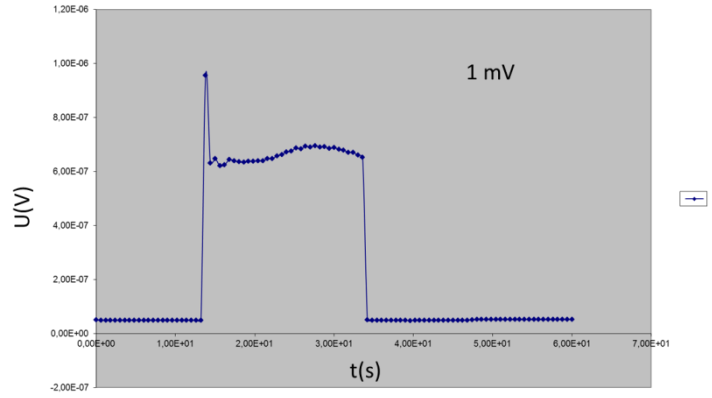

Figure 22. Current vs time under a polarization of 1 mV. UV excitation started at 12s and stopped at 33s.

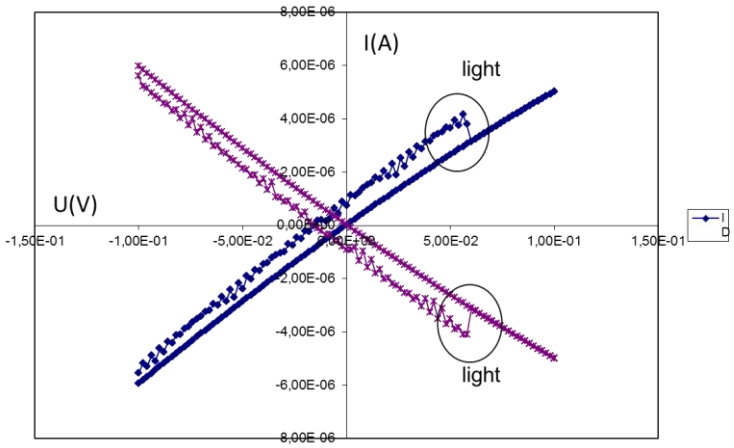

Figure 23. I(V) measurement in the dark and under UV excitation of the photoluminescent area of the sample.

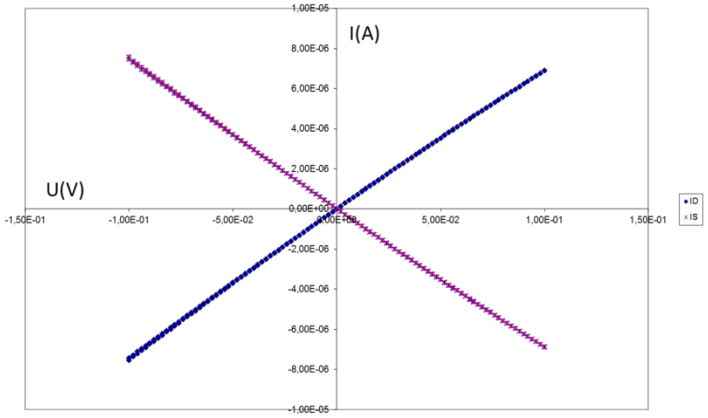

Figure 24. I(V) measurement in the dark and under UV excitation of a clean area of the silicon substrate.

The I(V) measurement of a non-luminescent part of the sample did not show a strong variation of the current under UV excitation. In fact, the effect of the UV excitation was slightly visible but was strongly lower compared to the photoluminescent area (Figure 25).

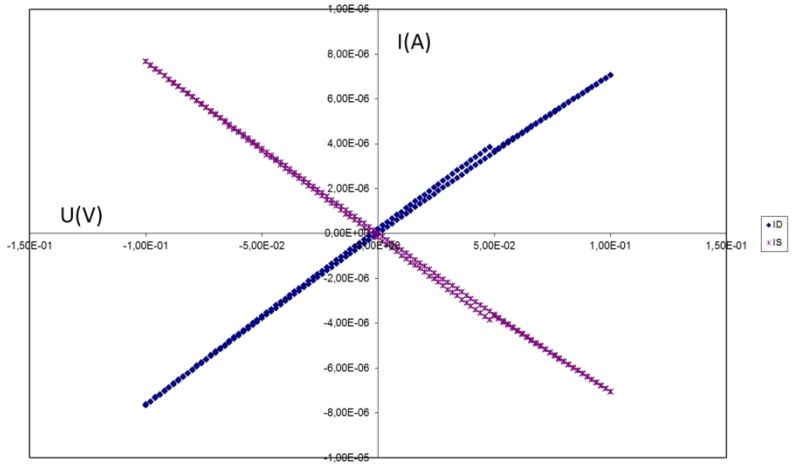

Figure 25. I(V) measurement in the dark and under UV excitation of a non-luminescent part of the sample.

The last experiment consisted of I(V) measurements of the photoluminescent part under halogen lamp excitation. The current variation was higher than in the case of UV excitation demonstration the promising potential of this material (Figure 26).

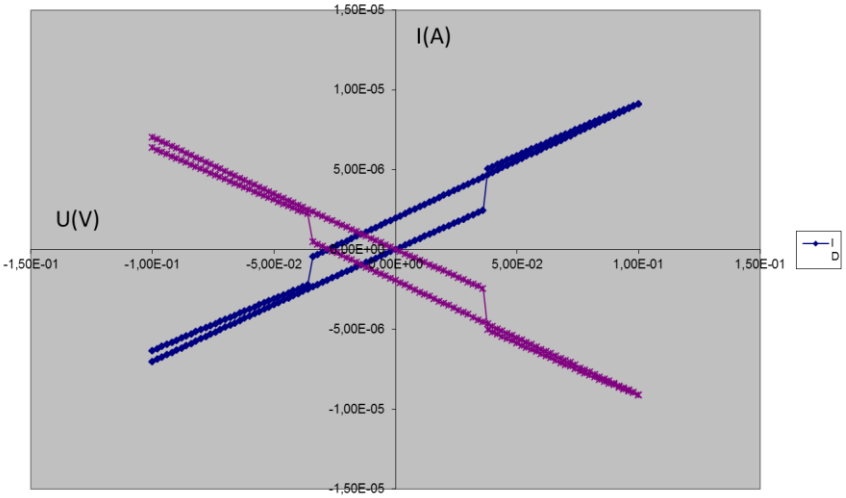

Figure 26. I(V) measurement in the dark and under halogen lamp excitation of a luminescent part of the sample

8. DISCUSSION

8.1. TEM studies of MWCNT – HfO_2, effects of sonication

Earlier studies confirm that sonication is an effective and simple method of dispersing nanotubes and increasing their solubility [68, 69, 70]. Duration of sonication is an important factor as prolonged exposure to sonication can seriously damage the nanotubes [71]. Ultimately, walls of CNTs will be destroyed and be converted into amorphous carbon nanofibers [72]. Sonication has been known to induce defects on the surface of the nanotubes [71] onto which nanoparticles can adhere [73]. On the bends the walls of CNTs are damaged mechanically. This could be an atom or several atoms, leaving its position and creating a vacancy in the graphene lattice structure. As a result, atoms in the graphene sheet will rearrange themselves to form pentagonal, heptagonal and octagonal patterns (or a combination of these) within the lattice, depending on the number of vacancies. In the case of a mono-vacancy, a pentagonal pattern is formed and one free dangling bond remains to react with its surroundings [28, 74]. These defect points provide anchor-sites for nanoparticle decoration of carbon nanotubes [75].

It was observed that before sonication, CNTs are covered in a layer of amorphous carbon and NPs would mainly attach to the tubes where they are mechanically damaged (bends, sidewall damages), in other words, where mechanically introduced functionalities were present. Further study showed how increasing sonication time improved the dispersion of both CNTs and HfO_2 particles. Dispersion can be attributed directly to sonication as the energy of ultrasonic waves overcomes the intermolecular forces, which causes the particles to stick together. Another effect of sonicating is the degradation of initial amorphous carbon on the CNTs surface. However, ultrasonic induces defects on CNT sidewalls and eventually will degrade a wall to a new layer of amorphous carbon. Based on our observation, a uniform amorphous layer is re-occurring at 90 minutes of sonication time and then at 180 minutes. On the other hand, sonication is a simple and an efficient way of functionalizing CNTs. Therefore it is important to find a balance between dispersion, damage, and functionalization and anchoring of the NPs. The aim is to obtain uniform anchoring of the CNT, with good nanoparticle and CNT dispersion. It is also necessary to get rid of excess pyrolytic amorphous carbon with minimal wall damage. Also, finding a good CNT – NP ratio in the mixture must be studied.

8.2. Concentration of HfO_2 nanoparticles in the material solution and carbon nanotube coverage

The calculations show that with the amounts of constituents used in this study, 12 mg of CNTs and HfO_2 nanoparticles, nanotube coverage value of 19,1% was achieved theoretically. In reality, this value cannot be reached due to the natural agglomeration of nanoparticles. Agglomeration is an inhibiting factor in the pursuit of uniform coverage of the CNTs. It is reported in earlier studies that sonication fractures other nanoparticle agglomerates but for HfO_2 nanoparticles no such study has been conducted. To overcome the phenomenon of agglomeration and finding the reason for this kind of persistent behaviour of NPs, further investigation is needed and will be performed.

8.3. Electrical measurements

Many tests were conducted for electrical characterization of MWCNT-HfO_2 nanohybrid. It was confirmed that MWCNTs are excellent electrical conductors. However, the first experiments were not conclusive and did not demonstrate photoconductive properties from the samples deposited on ceramic supports. The main hypotheses of this result were a too high concentration of CNTs compared to HfO_2 photoluminescent nanoparticle, a too low amount of materials on the support making the detection of photocurrent further complicated or an insufficiently high excitation source. The UV lamp used had a fiberoptic cable through which light was emitted and the beam of light was dispersed. A laser would have been more suitable for these experiments.

It was discussed that the capacitance tests were compromised by the UV resin that isolated CNTs, rendering their conductive properties to low levels. The experiment was granted all the best possibilities for succeeding: pure CNTs, 60 minute, 120 minute and 180 minute sonication time sample with good dispersion of CNTs and NPs, direct close-range illumination and more sensitive apparatus compared to the previous tests. Although some capacitance in the nanofarad range was measured, both in dark and with light, no significant result was achieved and possible photocapacitance property of this nanohybrid material has not been yet demonstrated at this stage.

Samples on the silicon wafers yielded the desired results – direct, measurable and reproducible measure of the light excitation on the sample. Firstly, the efforts were made to produce

photocurrent on the deposited sample with no conclusive results. Then, an area of highly luminescent properties was noticed on the silicon wafer. It was determined that this area contained a higher concentration of HfO_2 nanoparticles. This area exhibited blue-greenish luminescence that is characteristic to HfO_2 nanoparticles. Further interest was focused on this area and a photocurrent was measured under UV excitation and halogen lamp excitation. The measured current indicates the presence of nanotubes, although not observable to naked eye or even under the light microscope for that matter.

To confirm this result, the electrodes were placed on an area with no observable NPs or CNTs and no photocurrent was observed. Photocurrent was also observed on area with a very low content of both CNTs and HfO_2 nanoparticles, but the variation of the current under light excitation was remarkably lower. This indicates that on the right support material, even a very small amount of the solution will produce a photocurrent.

SUMMARY

The main objective of this master's thesis was to conduct a research on carbon nanotubes (CNT) combined with metal oxide nanoparticle (MONPS) nanohybrid materials and more particularly on CNT-HfO_2. These nanohybrid materials were synthesized via sonication and this study focused on the effects of the ultrasound on the CNT and how the ultrasounds affect both CNTs and HfO_2 nanoparticles. The roles of the ultrasounds were to first disperse the CNTs and then promote the anchoring of HfO_2 nanoparticles on the surface of the CNTs. The electrical properties and photoconductivity of the nanohybrid were also investigated via a collaboration with Minatec in Grenoble, France. The metal oxide nanoparticles used in this experiment were synthesized beforehand by Prof. Erwan Rauwel.

During synthesis process CNTs and HfO_2 nanoparticles were mixed together in 15 ml of ethanol with sonication time ranging from 0 to 180 min. A sample was taken from the main solution every 30 minutes for high resolution transmission electron microscopy study. From the initial mixture, a theoretical surface coverage of 19.1% was calculated. However, these calculations do not take into account the possibility of NPs to agglomerate and unbounded NPs. This aspect needs to be addressed in future studies.

The HRTEM study enables to highlight how the sonication duration affects the dispersion of materials, the modification of the surface of the CNTs and how HfO_2 nanoparticles are anchored on the surface of the CNTs. From this study, it was possible to highlight how simple ultrasound treatment is effective in terms of dispersion of the materials, CNTs functionalization and NPs anchoring. At the first stage of the sonication treatment, a depletion of the amorphous layer on the surface of the CNTs was observed and did not promote an efficient NPs coverage on their surface. However, from duration of 30 min, an improvement of the anchoring of NPs was observed. However, more defects in the structure and on the surface of the CNTs were observed.

The electrical measurements showed good electrical conductivity of the nanohybrid. In addition, these electrical measurements enable to demonstrate photocurrent and photocapacitance properties under UV illumination. This preliminary study showed that this nanohybrid appears to be a promising material for applications in the field of photovoltaics.

In summary, this preliminary study proved that the ultrasonic treatment is an effective method for introducing functionalities to non-functionalized CNTs and anchoring MONPS on their

surface. Moreover, this study showed that UV excitation induces a photocurrent in this nanohybrid. The complete understanding of this material in the frame of future applications needs more investigation and will be the subject of a future research project for a PhD student.

CONCLUSION

In this master's thesis an investigation on the synthesis and characterization of nanohybrids composed of carbon nanotubes combined with HfO_2 metal oxide nanoparticles was conducted. The synthesis of this CNT-HfO_2 nanohybrid was done via sonication treatment and the effect of the duration of sonication treatment on the nanostructure was more particularly investigated. In a second approach, electrical measurements under light excitation were carried out to evaluate the potential of these nanohybrids for photovoltaic applications.

Mixture of CNT-HfO_2 was composed of 10.8 mg of CNTs and 10.32 mg of HfO_2 nanoparticles which theoretical should correspond to 19.1% coverage of CNTs by the NPs. This study showed that the duration of the sonication treatment promotes the anchoring of the nanoparticles on the surface of non-functionalized CNTs, but also affects the nanostructure of the CNTS and more particularly induces an amorphisation of the surface of the CNTs. It was observed that at the HfO_2 NPs first attach on the defects present on the surface of the CNTs, such as kinks and bends even without sonication. After 30 min treatment, it was also observed that the HfO_2 NPS also are bonded all along the surface of the CNTs, but attach preferentially on the surface defects. The present study only focused on a theoretical coverage of 19% and needs to be renewed with other coverage ratio. In fact, we showed that it is necessary to find compromise between promotion of the anchoring and the CNT surface modification. Therefore further investigation is needed to identify the optimal sonication duration for different CNT-HfO_2 ratio and will be the scope a future PhD research project.

The first electrical characterizations have shown that even after an intense sonication treatment, the CNTs retained their electrical properties. It has also been demonstrated for the first time that the CNT-HfO_2 nanohybrid exhibits photoconductivity properties when exposed to UV light and halogen lamp, which makes them of high interest for applications.

This master's thesis investigated the structural and photoluminescence properties of a new CNTs-HfO_2 nanohybrid. According to the present findings, this nanohybrid appears to be a promising material for future photovoltaic applications. However, further research investigations and studies have to be performed for having a better understanding of this material and the improvement of its properties.

ACKNOWLEDGEMENTS

First of all I would like to thank my supervisors Prof. Erwan Rauwel and Dr. Protima Rauwel for their professionalism, knowledge, guidance and support over the period of writing this thesis. This project would not have been possible without them and I do not have enough words to express my gratitude to them. Dr. Frédérique Ducroquet from MINATEC, Grenoble, France for all her help and guidance in electrical measurements carried out via the PARROT program exchange during my stay in Grenoble. I would like to thank all the staff at Tallinn University of Technology, Tartu College for supportive information and understanding. I also want to acknowledge all my friends, fellow students and family who provided me with all kind of support, especially Siim, Martin, Sten-Oliver, Artur, Helen, Triin and Anneli.

REFERENCES:

1. There's Plenty of Room at the Bottom. An Invitation to Enter a New Field of Physics. [WWW] http://www.zyvex.com/nanotech/feynman.html
2. Definition – What is nanotechnology? [WWW] http://www.nanowerk.com/nanotechnology/introduction/introduction_to_nanotechnology_1.php
3. NNI: Leading to the Next Industrial Revolution, 2000. [WWW] https://www.whitehouse.gov/files/documents/ostp/NSTC%20Reports/NNI2000.pdf
4. NNI Budget 2016. [WWW] http://www.nano.gov/sites/default/files/pub_resource/nni_fy16_budget_supplement.pdf
5. Ten things you should know about nanotechnology. [WWW] http://www.nanowerk.com/nanotechnology/ten_things_you_should_know_6.php
6. Global Funding Of Nanotechnologies & Its Impact, 2011. [WWW] http://cientifica.com/wp-content/uploads/downloads/2011/07/Global-Nanotechnology-Funding-Report-2011.pdf
7. P. Lin, J. Moor, J. Weckert. Nanoethics. The ethical and social implications of nanotechnology. Wiley, 2007
8. Nanotechnology: Clean Energy and Resources for the Future. [WWW] https://www.foresight.org/impact/whitepaper_illos_rev3.PDF
9. The History of Carbon Nanotubes – Who Invented The Nanotube? [WWW] http://nanogloss.com/nanotubes/the-history-of-carbon-nanotubes-who-invented-the-nanotube/#axzz3Z9zGLayA
10. R. - R. Bi, X. – L. Wu, F.- F. Cao, L.-Y. Jiang, Y. – G. Guo and L. – J. Wan, Highly Dispersed RuO2 Nanoparticles on Carbon Nanotubes: Facile Synthesis and Enhanced Supercapacitance Performance. J. Phys. Chem. C, 114 (6), pp 2448–2451, 2010 [*Online*] ACS Publications
11. S.-Y. Lee, S.-J. Park, TiO2 photocatalyst for water treatment applications, Journal of Industrial and Engineering Chemistry Volume 19, Issue 6, Pages 1761–1769, 2013 [*Online*] ScienceDirect, Elsevier

12. A. Jorio, M.S. Dresselhaus, G. Dresselhaus. Carbon Nanotubes: Advanced Topics in the Synthesis, Structure, Properties and Applications. Springer Science & Business Media, 2007
13. Carbon Nanotubes Technology Overview. [WWW] http://www.nanoscience.com/products/carbon-nanotube-synthesis/technology-overview/
14. Who should be given the credit for the discovery of carbon nanotubes? [WWW] http://nanotube.msu.edu/HSS/2006/1/2006-1.pdf
15. M. Terrones, Science and Technology of the Twenty-first Century: Synthesis, Properties and Applications of Carbon Nanotubes. Annu. Rev. Mater.Res. 33:419–501,2003. [*Online*]
16. Sporting Goods with Nanotechnology. [WWW] http://www.understandingnano.com/sporting_goods.html
17. M. Meyyappan, Carbon Nanotubes Science and Applications, CRC Press, 2005.
18. Carbon Nanotube-Coated Filters Foil Bacteria. Chemical and Engineering News. [WWW] http://cen.acs.org/articles/91/web/2013/02/Carbon-Nanotube-Coated-Filters-Foil.html
19. Filtering Water with Acoustics Nanotube Technology. [WWW] https://www.nasa.gov/centers/johnson/techtransfer/technology/MSC-24180-1_Water-Filtering-Device_prt.htm
20. O. Yildiz, Philip D. Bradford, Aligned carbon nanotube sheet high efficiency particulate air filters. Carbon, Volume 64, November 2013, Pages 295–304. [*Online*] ScienceDirect
21. Nano-enhanced Wholesale Technologies. [WWW] http://www.nano-enhanced-wholesale-technologies.com/faq/carbon-forms.htm
22. Prabhakar R. Bandaru, Electrical Properties and Applications of Carbon Nanotube Structures. Journal of Nanoscience and Nanotechnology Vol.7, 1–29, 2007 [*Online*] American Scientific Publishers
23. Nanotube Cables Hit a Milestone: As Good as Copper. MIT Technology Review. [WWW] http://www.technologyreview.com/news/425468/nanotube-cables-hit-a-milestone-as-good-as-copper/

24. I. Stemmler and C. Backes, Absorption Spectroscopy as a Powerful Technique for the Characterization of Single-Walled Carbon Nanotubes. PerkinElmer GmbH, 2013. [WWW] http://www.perkinelmer.com/cmsresources/images/44-156326wht_011513_01_lambda_1050single-walledcarbonnanotubes.pdf
25. M. E. Itkis, D. E. Perea, R. Jung, S. Niyogi, and R. C. Haddon, Comparison of Analytical Techniques for Purity Evaluation of Single-Walled Carbon Nanotubes. J. Am. Chem. Soc. 9 Vol. 127, No. 10, 2005 [Online] ACS Publications http://pubs.acs.org/doi/pdf/10.1021/ja043061w
26. CNTs absorption spectra. [WWW] http://upload.wikimedia.org/wikipedia/commons/4/4d/CNTabsorption.jpg
27. L. Chen, H. Xie and W. Yu, Functionalization Methods of Carbon Nanotubes and Its Applications, Carbon Nanotubes Applications on Electron Devices, p. 213-232, 2011 [*Online*] InTech.
28. Philip G. Collins, Oxford Handbook of Nanoscience and Technology: Frontiers and Advances. Oxford Univ. Press. 2009
29. M. Zhang and J. Li, Carbon nanotube in different shapes. Materials Today, Volume 12, Issue 6, Pages 12–18, 2009 [*Online*] ScienceDirect, Elsevier
30. Y. Liu, Y. Zhao, B. Sun and C. Chen, Understanding the Toxicity of Carbon Nanotubes, Accounts of Chemical Research Vol. 46, No. 3, pages 702–713, 2013 [*Online*] ACS Publications
31. S.K. Smart, A.I. Cassady, G.Q. Lu and D.J. Martin, The biocompatibility of carbon nanotubes. Carbon, Volume 44, Issue 6, pages 1034–1047, 2006 [*Online*] ScienceDirect, Elsevier
32. J. M. Wörle-Knirsch, K. Pulskamp and H. F. Krug, Oops They Did It Again! Carbon Nanotubes Hoax Scientists in Viability Assays, Nano Lett., 2006, 6 (6), pp 1261–1268. [*Online*] ACS Publications
33. Victor E. Henrich and P. A. Cox, The Surface Science of Metal Oxides, Cambridge University Press, 1996
34. M. Fernández-Garcia, J. A. Rodriguez, Metal Oxide Nanoparticles, 2007. [WWW] http://www.bnl.gov/isd/documents/41042.pdf
35. W. Cao, Synthesis of Nanomaterials by High Energy Ball Milling [WWW] http://www.understandingnano.com/nanomaterial-synthesis-ball-milling.html

36. T. P. Yadav, R. M. Yadav, D. Pratap Singh, Mechanical Milling: a Top Down Approach for the Synthesis of Nanomaterials and Nanocomposites, Nanoscience and Nanotechnology, 2012. [*Online*] Scientific & Academic Publishing
37. H. Hayashi and Y. Hakuta, Hydrothermal Synthesis of Metal Oxide Nanoparticles in Supercritical Water, Materials 2010, 3(7), 3794-3817. [*Online*] MDPI
38. K. M. Ørnsbjerg Jensen, Watching Materials Form: Particle Formation and Growth in Hydrothermal Synthesis, PhD Dissertation, 2013. [*Online*] https://www.maxlab.lu.se/files/PhD_dissertation_KirstenJensen_reducedsize%281%29.pdf
39. M. Niederberger and N. Pinna, Metal Oxide Nanoparticles in Organic Solvents, Engineering Materials and Processes, 2009. Springer.
40. M. Niederberger and G. Garnweitner, Organic Reaction Pathways in the Nonaqueous Synthesis of Metal Oxide Nanoparticles, Chemistry - A European Journal, volume 12, Issue 28, 2006 [*Online*] Wiley Online Library
41. Hanna L. Karlsson , Pontus Cronholm , Johanna Gustafsson and Lennart Möller, Copper Oxide Nanoparticles Are Highly Toxic: A Comparison between Metal Oxide Nanoparticles and Carbon Nanotubes, Chem. Res. Toxicol., 2008, 21 (9), pp 1726–1732. [*Online*]
42. H. Jeng, J. Swanson, Toxicity of metal oxide nanoparticles in mammalian cells. J. Environ. Sci. Health A Tox. Hazard Subst. Environ. Eng. 2006; 41(12):2699-711. [*Online*]
43. J. A. Fielda, A. L. Velascoa, S. A. Boitanob, F. Shadmana, B. d. Ratnerc, C. Barnesc, R. Sierra-Alvarez, Cytotoxicity and physicochemical properties of hafnium oxide nanoparticles. Chemosphere, Volume 84, Issue 10, September 2011, Pages 1401–1407 [*Online*] ScienceDirect, Elsevier
44. K. Byrappa, A. S. Dayananda, C. P. Sajan, B. Basavalingu, M. B. Shayan, K. Soga, M. Yoshimura, Hydrothermal preparation of ZnO:CNT and TiO_2:CNT composites and their photocatalytic applications. J Mater Sci (2008) 43:2348–2355. [*Online*] Springer
45. Z. Lia, B. Gaoa, G. Z. Chena, R. Mokayab, S. Sotiropoulosc, G. L. Puma, Carbon nanotube/titanium dioxide (CNT/TiO2) core–shell nanocomposites with tailored shell thickness, CNT content and photocatalytic/photoelectrocatalytic properties. Applied Catalysis B: Environmental, Volume 110, 2 November 2011, Pages 50–57. [*Online*] ScienceDirect, Elsevier

46. C. Hung, H. – C. Wen, Y. – C. Lai, S. – H. Chang, W. – C. Chou and W. – K. Hsu, ZnO – coated Carbon Nanotubes: Inter - Diffusion of Carboxyl Groups and Enhanced Photocurrent Generation. Chem. Phys. Chem. 2015, 16, 812 – 816. [*Online*]
47. P. Rauwel, E. Rauwel, C. Persson, M. F. Sunding, and A. Galeckas. One step synthesis of pure cubic and monoclinic HfO_2 nanoparticles: Correlating the structure to the electronic properties of the two polymorphs. J. Appl. Phys. 112, 104107 (2012). [*Online*]
48. Short and Simple Guide to X-ray Diffraction. [WWW] http://dnaandsocialresponsibility.blogspot.com/2011/03/short-and-simple-ish-guide-to-x-ray.html
49. P. Rauwel, E. Rauwel, C. Persson, M. F. Sunding, and A. Galeckas, One step synthesis of pure cubic and monoclinic HfO2 nanoparticles: Correlating the structure to the electronic properties of the two polymorphs
50. Electron Microscopy Tutorial. [WWW] http://advanced-microscopy.utah.edu/education/electron-micro/
51. The electron wavelength. [WWW] http://www.ammrf.org.au/myscope/tem/background/concepts/imagegeneration/wavelength.php
52. Image Formation in the TEM. [WWW] http://www.asu.edu/courses/phs208/patternsbb/PiN/rdg/elmicr/elmicr-tem.gif
53. NANOCYL™ NC7000 series - Product Datasheet. [WWW] http://www.matweb.com/search/datasheet.aspx?matguid=94228642b4eb40d882658fb7853f240b&ckck=1
54. M. Kumar and Y. Ando. Chemical Vapor Deposition of Carbon Nanotubes: A Review on Growth Mechanism and Mass Production, Journal of Nanoscience and Nanotechnology Vol. 10, 3739–3758, 2010
55. M. Pumera, Carbon Nanotubes Contain Residual Metal Catalyst Nanoparticles even after Washing with Nitric Acid at Elevated Temperature Because These Metal Nanoparticles Are Sheathed by Several Graphene Sheets, Langmuir 2007, 23, 6453-6458
56. D. Cunningham, A First-Principles Examination of Dopants in HfO2. Honors Scholar Theses, University of Connecticut. 2014. [*Online*]

57. FCC unit cell Figure. [WWW] http://assets.openstudy.com/updates/attachments/4f466f3fe4b065f388ddf1bf-jfraser-1330018875028-cusersjfraserdesktopface_centered_cubic2.jpg
58. AFM working principle. [WWW] http://www.microworldreflections.com/uploads/5/6/9/5/5695252/9630668_orig.jpg
59. S.J. Chunga, J.P. Leonarda, I. Nettleshipa, J.K. Leea, Y. Soongb, D.V. Martellob, M.K. Chyua, Characterization of ZnO nanoparticle suspension in water: Effectiveness of ultrasonic dispersion, Powder Technology, Volume 194, Issues 1–2, 25 August 2009, Pages 75–80. [*Online*]
60. Richard D. West, Vivak M. Malhotra, Rupture of Nanoparticle Agglomerates and Formulationof Al_2O_3-Epoxy Nanocomposites Using UltrasonicCavitation Approach: Effects on the Structural andMechanical Properties, Polymeer Engineering and Science, 2006, pages 426 – 430. [*Online*]
61. K.Sato, J.-G. Li, H. Kamiya and T. Ishigaki, Ultrasonic Dispersion of TiO2 Nanoparticles in Aqueous Suspension, Journal of the American Ceramic Society, Volume 91, Issue 8, pages 2481–2487, 2008. [*Online*]
62. A. Rinaldi, B. Frank, D. S. Su, S. B. Abd Hamid and R. Schlogl, Facile Removal of Amorphous Carbon from Carbon Nanotubes by Sonication, Chem. Mater. 2011, 23, 926–928. [*Online*]
63. A. Koshio, M. Yudasaka, M. Zhang, S. Iijima, A Simple Way to Chemically React Single-Wall Carbon Nanotubes with Organic Materials Using Ultrasonication, Nano Letters, Vol. 1, No. 7, 2001. [*Online*]
64. B. Flint and K. S. Suslick, Temperature of Cavitation, Science, New Series, Volume 253, Issue 5026, 1397-1399, 1991. [*Online*]
65. F. Müller, W. Peukert, R. Polke, F. Stenger, Dispersing nanoparticles in liquids, International Journal of Mineral Processing Volume 74, Supplement, 10 December 2004, Pages S31–S41. [*Online*]
66. G. Cao, Y. Wang, Nanostructures and Nanomaterials: Synthesis, Properties, and Applications 2nd edition, 2011
67. W. Huang, Y. Lin, S. Taylor, J. Gaillard, A. M. Rao, and Y.-P. Sun, Sonication-Assisted Functionalization and Solubilization of Carbon Nanotubes, NANO LETTERS Vol. 2, No. 3 231-234, 2002. [*Online*]
68. Y. Kun, Y. Z. Li, J. Qing Feng, Y. Ren Liang, J. Wei and L. Dao Hui, Sonication-assisted dispersion of carbon nanotubes in aqueous solutions of the anionic surfactant

SDBS: The role of sonication energy , Materials Science 2013 Vol.58 No.17: 2082–2090. [*Online*]

69. Y. Huang and Eugene M. Terentjev, Dispersion of Carbon Nanotubes: Mixing, Sonication, Stabilization, and Composite Properties, Polymers 2012, 4, 275-295
70. Dumée, K. Sears, J. Schütz, N. Finn, M. Duke and Stephen Gray, Influence of the Sonication Temperature on the Debundling Kinetics of Carbon Nanotubes in Propan-2-ol, Nanomaterials 2013, 3, 70-85. [*Online*]
71. P.-C. Ma, N. A. Siddiqui, G. Marom, J.-K. Kim, Dispersion and functionalization of carbon nanotubes for polymer-based nanocomposites: A review, Elsevier Volume 41, Issue 10, October 2010, Pages 1345. [*Online*]
72. K. Mukhopadhyay, C. D. Dwivedi, G. N .Mathur, Conversion of carbon nanotubes to carbon nanofibers by sonication, Carbon 40 (2002) 1369 –1383. [*Online*]
73. D. Yang, J.-F. Rochette and E. Sacher, Functionalization of Multiwalled Carbon Nanotubes by Mild Aqueous Sonication, J. Phys. Chem. B 2005, 109, 7788-7794. [*Online*]
74. D. P. Hashim, N. T. Narayanan, J. M. Romo-Herrera, D. A. Cullen, M. Gwan Hahm, P. Lezzi, J. R. Suttle, D. Kelkhoff, E. Muñoz-Sandoval, S.i Ganguli, A. K. Roy, D. J. Smith, R. Vajtai, B. G. Sumpter, V. Meunier, H. Terrones, M. Terrones & P. M. Ajayan, Covalently bonded three-dimensional carbon nanotube solids via boron induced nanojunctions. Scientific Reports 2, Article number: 363, 2012. . [*Online*]
75. Sammalkorpi et al. , Mechanical properties of carbon nanotubes with vacancies and related defects, Physical Review B 70, 245416 (2004) . [*Online*]